Basin Research

IAS EAGE

Basin Research (2016) 1–20, doi: 10.1111/bre.12229

An integrated model of clastic injectites and basin floor lobe complexes: implications for stratigraphic trap plays

Sarah Louise Cobain, David Mark Hodgson, Jeff Peakall and Michelle Nicole Shiers

School of Earth and Environment, University of Leeds, Leeds, UK

ABSTRACT

Injectites sourced from base-of-slope and basin-floor parent sandbodies are rarely reported in comparison to submarine slope channel systems. This study utilizes the well-constrained palaeogeographic and stratigraphic context of three outcrop examples exposed in the Karoo Basin, South Africa, to examine the relationship between abrupt stratigraphic pinchouts in basin-floor lobe complexes, and the presence, controls, and character of injectite architecture. Injectites in this palaeogeographic setting occur where there is: (i) sealing mudstone both above and below the parent sand to create initial overpressure; (ii) an abrupt pinchout of a basin-floor lobe complex through steep confinement to promote compaction drive; (iii) clean, proximal sand beds aiding fluidization; and (iv) a sharp contact between parent sand and host lithology generating a source point for hydraulic fracture and resultant injection of sand. In all outcrop cases, dykes are orientated perpendicular to palaeoslope, and the injected sand propagated laterally beneath the parent sand, paralleling the base to extend beyond its pinchout. Understanding the mechanisms that determine and drive injection is important in improving the prediction of the location and character of clastic injectites in the subsurface. Here, we highlight the close association of basin-floor stratigraphic traps and sub-seismic clastic injectites, and present a model to explain the presence and morphology of injectites in these locations.

INTRODUCTION

Improvements in subsurface imaging quality in recent years have led to increased recognition and understanding of the impact of injectites on the architecture and fluid flow of sedimentary basin-fills. However, the distribution of subseismic scale injectites and their relationship with those of a seismic-scale are poorly understood (Hurst & Cartwright, 2007). The literature is dominated by examples of clastic injectites that are associated with primary deposits on a slope setting, such as deep marine channel-fills (Hiscott, 1979; Dixon *et al.*, 1995; Rowe *et al.*, 2002; Parize & Friès, 2003; Duranti & Hurst, 2004; Huuse *et al.*, 2005; Diggs, 2007; Duranti, 2007; Frey-Martínez *et al.*, 2007; Hamberg *et al.*, 2007; Jackson, 2007; Jonk *et al.*, 2007; Surlyk *et al.*, 2007; Vigorito *et al.*, 2008; Kane, 2010; Svendsen *et al.*, 2010; Szarawarska *et al.*, 2010; Jackson *et al.*, 2011; Løseth *et al.*, 2013; Morton *et al.*, 2014; Bain & Hubbard, 2016) and intraslope lobes (Monnier *et al.*, 2014; Yang & Kim, 2014; Spychala *et al.*, 2015). In cases where the parent sand cannot be directly constrained, regional context still suggests that injectites were originally sourced from a submarine slope sandbody (e.g. Panoche complex: Vigorito *et al.*, 2008) or slope channel-fills (e.g. Chile: Hubbard *et al.*, 2007). These depositional environments commonly provide the key conditions for clastic injection, including: (i) pore pressure in parent sandbody higher than that within the mud-prone host strata (Lorenz *et al.*, 1991; Cosgrove, 2001; Jolly & Lonergan, 2002), and (ii) clean, fine to very fine unconsolidated sand that is most susceptible to fluidization and grain transport (Richardson, 1971; Jolly & Lonergan, 2002). In contrast, injectites demonstrably sourced from base of slope and basin floor sandbodies have rarely been documented (Cobain *et al.*, 2015).

In sedimentary basins, lithology is the principle control on basin wide fluid migration (Bjørlykke, 1993; Jonk *et al.*, 2005a), and in the absence of clastic injectites fractures and faults form the most efficient conduits for fluid flow (Chapman, 1987; Knipe *et al.*, 1998; Aydin, 2000). However, clastic injectites create additional fluid flow pathways, and their impact depends on their timing and location (e.g. Hurst *et al.*, 2003; Jonk, 2010; Ross *et al.*, 2014). Net migration of fluids, including water and hydrocarbons, into an unconsolidated sandbody can provide the overpressure and trigger mechanism needed for sands to fluidize and inject (Vigorito & Hurst, 2010; Bureau *et al.*, 2014). Post-injection, sandstone dykes and sills can act as fluid flow conduits for hydrocarbon leakage (Jonk, 2010) until cementation, at which point injectites become fluid flow baffles and barriers. Later, reactivation of clastic injectites as fluid flow conduits can occur

Correspondence: S. L. Cobain, School of Earth and Environment, University of Leeds, Leeds LS2 9JT, UK. E-mail: Sarah.L.Cobain@gmail.com

through preferential brittle deformation of competent sandstones within a low-competence (majority mudstone) host rock (Jonk *et al.*, 2005a).

For the first time, we present examples of injectites at outcrop where the palaeogeographic and stratigraphic context of the basin-floor parent sandstone lobe deposits are well constrained. We address the following objectives: (i) to document the architecture and character of injectites in basin-floor settings in terms of thickness and morphology in relation to parent sand, (ii) to investigate the association between the architecture and character of the basin-floor parent sandbody as a control on the location and orientation of injectites, (iii) to construct an integrated model of clastic injectites in basin-floor settings, (iv) to consider the role of basin-wide fluid flow pre-, syn- and post-injection, and (v) to discuss the association and implication for subsurface stratigraphic trap plays and the presence of injectites.

GEOLOGICAL SETTING

The Karoo Basin has long been interpreted as a retro-arc foreland basin that formed on the southern margin of the Gondwana palaeocontinent behind a magmatic arc and fold-and-thrust belt (Johnson, 1991; Visser & Praekelt, 1996; Catuneanu *et al.*, 1998; Johnson *et al.*, 2006). However, more recent studies suggest subsidence during the Permian was driven by mantle flow and foundering of basement blocks coupled to subduction of the palaeo-Pacific Plate to the south, pre-dating the Cape Orogeny (Tankard *et al.*, 2009). The Ecca Group, a siliciclastic succession, was deposited in the southwestern Karoo Basin during the Permian (Flint *et al.*, 2011). This part of the basin is subdivided into the Laingsburg and Tanqua depocentres (Fig. 1a), and this study focusses on three outcrop examples of exhumed clastic injectites hosted in deep water strata of the Ecca Group across these depocentres (Fig. 1c and d).

The Tanqua depocentre infill comprises 1.3 km of deep-water sediments (Hodgson *et al.*, 2006) of the upper Ecca Group (Tierberg and Skoorsteenberg formations; Wickens, 1994; Wickens & Bouma, 2000) overlain by submarine slope and shelf-edge deltaic deposits (Kookfontein Formation; Wild *et al.*, 2009) (Fig. 1b). The 400 m thick Skoorsteenberg Formation comprises four sand-prone basin-floor fans (Fans 1-4) that are separated by laterally extensive fine grained intervals (Hodgson *et al.*, 2006) and overlain by a 100 m thick channelized slope succession (Unit 5) (Fig. 1b). The adjacent Laingsburg depocentre was infilled by a 1.8 km thick shallowing upward succession from distal and proximal basin-floor (Vischkuil and Laingsburg formations, respectively; van der Merwe *et al.*, 2010; Flint *et al.*, 2011) through leveed slope-channels (Fort Brown Formation; Kane & Hodgson, 2011; Morris *et al.*, 2014) to shelf-edge and shelf deltas (Waterford Formation; Jones *et al.*, 2015) (Fig. 1b). Sand-prone Units C to G, which comprise the Fort Brown Formation (Fig. 1b), have been mapped over 2500 km^2 (van der Merwe *et al.*, 2014), and are separated by regional mudstones interpreted to represent clastic input shutdown due to relative sea level rise (Di Celma *et al.*, 2011; Flint *et al.*, 2011; Fig. 1b).

METHODOLOGY AND DATASET

Three outcrops were studied in detail; Bizansgat (Tanqua depocentre: injectites associated with Fan 3) (Figs 1-4), Zoutkloof and Slagtersfontein (Laingsburg depocentre: injectites associated with Unit C, Subunits C1 and C2) (Figs 1 and 5-7). Recognition criteria of injectites in the Karoo Basin include cross-cutting relationships, direct connection to overlying sandstones, preserved patterns on fracture surfaces of injectite margins, such as plumose patterns and parallel ridges, and blistered and mudstone clast-rich surfaces (c.f. Cobain *et al.*, 2015). Field-based sedimentological and stratigraphic observations include logged vertical profiles, photo-panels, and dip and strike data of bedding and injectites. Physical correlation of individual beds and injectites between logs enabled the changing position of injectites with respect to host stratigraphy to be constrained from cm to km scale, which can be subtle.

OUTCROP DATA

Bizansgat; Tanqua depocentre

Fan architecture

The depositional architecture of Fan 3 is well-constrained due to extensive outcrop study (e.g. Johnson *et al.*, 2001; Prélat *et al.*, 2009; Jobe *et al.*, 2012; Hofstra *et al.*, 2015), and behind-outcrop research boreholes (Hodgson *et al.*, 2006; Luthi *et al.*, 2006). Research borehole NB4 (Fig. 2) confirmed that Fans 1 and 2 are not present in this part of the study area (Hodgson *et al.*, 2006; Luthi *et al.*, 2006). Fan 3 pinches out northward (down dip) from 65 m thick over 30 km (~2.2 m km^{-1} thinning rate) (Hodgson *et al.*, 2006). Southward (oblique up dip) thinning is more abrupt, and Fan 3 thins to <2 m thick over a distance of 3 km (~22 m km^{-1} thinning rate) (Hodgson *et al.*, 2006; Oliveira *et al.*, 2009). The fan has been interpreted as a basin-floor lobe complex comprising at least six sand-rich lobe deposits (Prélat *et al.*, 2009; Hofstra *et al.*, 2017) and the most updip exposures at Ongeluks River are interpreted as channelized lobe deposits in a base-of-slope setting (Hofstra *et al.*, 2015, 2017). Beds at the southward pinchout of the lobe complex remain sand dominated, between 5 and 30 cm in thickness, and display some planar and ripple lamination. Across the Ongeluks River locality to the pinchout, the upper beds of Fan 3 remain thinner bedded than those below. Fan 4 also thins

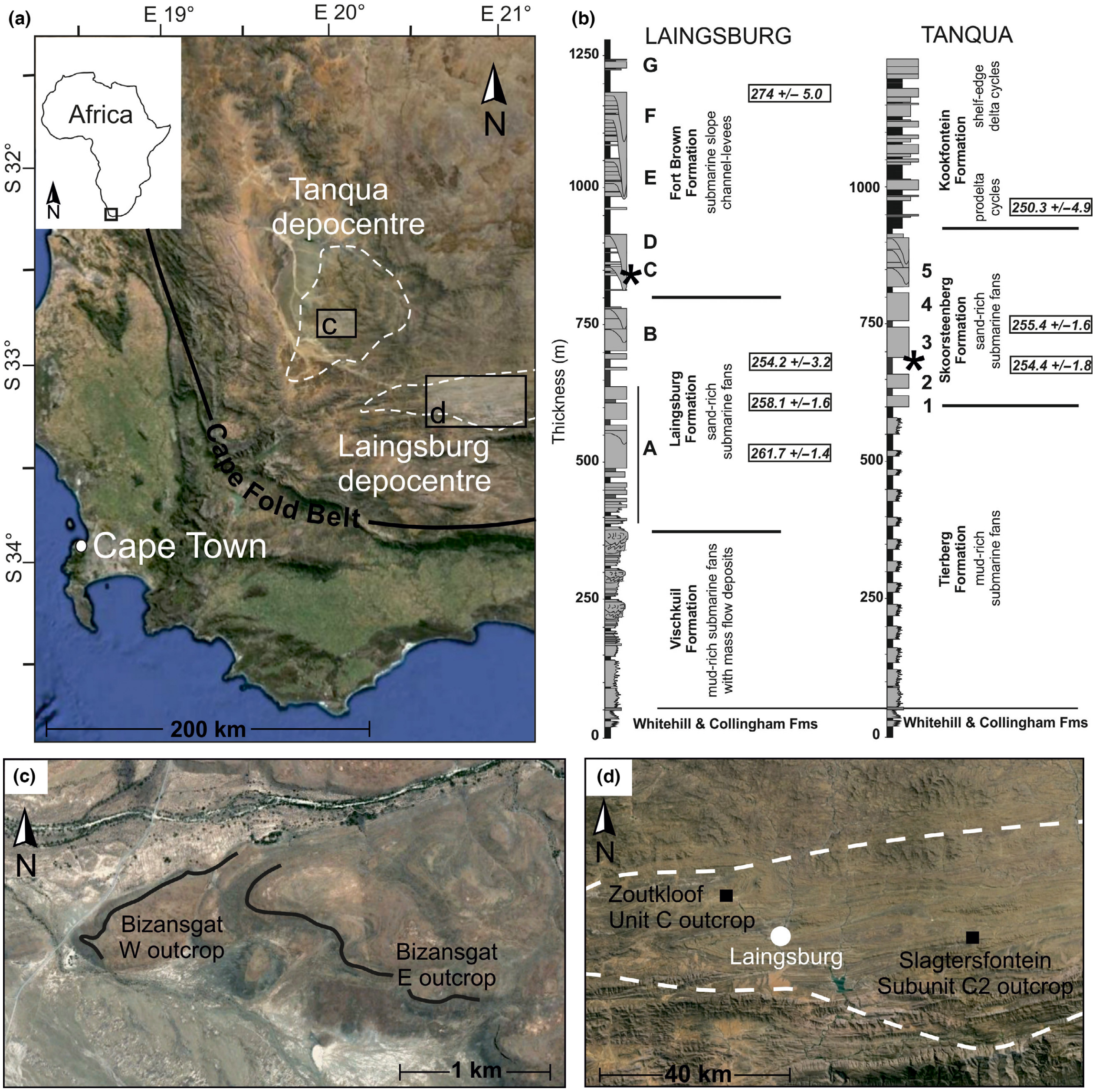

Fig. 1. (a) GoogleEarth image of SW Karoo Basin with Tanqua and Laingsburg depocentres outlined. Insets show outcrop localities in each depocentre, respectively. (b) Summary stratigraphic logs of Laingsburg depocentre, letters A-G refer to Units A-G (Flint *et al.*, 2011) and Tanqua depocentre, numbers 1-4 refer to Fans 1-4, whilst 5 refers to Unit 5, a 100 m thick channelized slope succession (Hodgson *et al.*, 2011b). Location of injectites, studied in the present paper, denoted by asterisks. Ages from U-Pb zircon analysis of volcanic ashes (see Fildani *et al.*, 2007; McKay *et al.*, 2015) are displayed in boxes as Ma. (c) Tanqua depocentre study area. (d) Laingsburg depocentre study areas.

abruptly southward, although the mudstone between Fan 3 and 4 maintains a constant thickness (Oliveira *et al.*, 2009). At the Ongeluks River locality (Fig. 2), Fan 3 is 65 m thick and is composed of clusters of sand-rich channel-fills, interpreted as base-of-slope channel complexes (Sullivan *et al.*, 2000; Luthi *et al.*, 2006) that incise lobe deposits (Hofstra *et al.*, 2017). The channels are orientated dominantly towards the NE (Luthi *et al.*, 2006; their Fig. 11) with variations to the N and E (Hodgetts *et al.*, 2004). The palaeoslope feeding Fan 3 was NE-facing (Hodgson *et al.*, 2006). The abrupt southeastward pinchout is interpreted to be due to lateral onlap, forming a sharp-based contact, onto a confining NE-SW-trending and NW-facing slope (Oliveira *et al.*, 2009) in a proximal base-of-slope setting (Hodgson *et al.*, 2006).

Injectites below Fan 3

Injectites exposed in the Bizansgat area of the Tanqua depocentre reported here occur in mudstones below Fan 3 (Fig. 1b) in the most proximal exposures to the south of the outcrop belt (Fig. 2). The nature of the outcrop

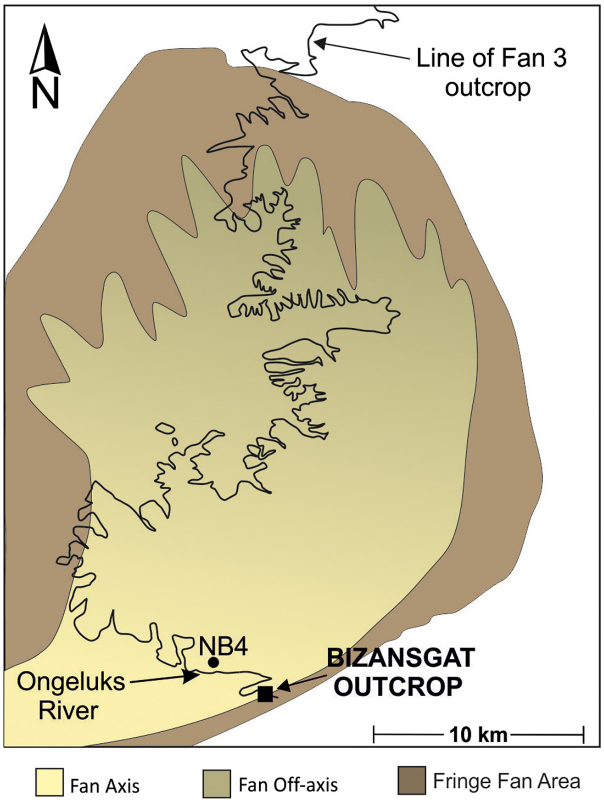

Fig. 2. Palaeogeography of Fan 3 (adapted from Hofstra *et al.*, 2015) with location of NB4 core and Ongeluks River section.

means that the 3D geometry of the larger injectites exposed in the mudstone below Fan 3 can be constrained. Locally, a single main laterally extensive ~1 m thick clastic sill steps up to the south and east to form a discordant relationship with the stratigraphy (Fig. 3a). Figure 4a and b shows the outcrop extent of the main stepped sill, which connects to at least three 0.4–0.6 m wide sub-vertical dykes that connect to the base of Fan 3 over a vertical distance of between 3 and 7 m. Steps on this sill are curvilinear along strike (Fig. 4), forming crescent-like geometries up to 200 m across and are no more than 1 m in vertical height. Propagating below the main sill are several thinner dykes (<0.2 m) that extend <6 m vertically, and bifurcate and taper out. Ridges that are orientated sub-horizontally with the host strata (Fig. 3c) mark the margins of these dykes. Margin structures on both the main stepped sill, and connecting dykes, include plumose patterns on fracture surfaces, parallel ridges, mudstone clast-rich surfaces and planar surfaces (Fig. 3b–f). The average strike of the steps is WNW-ESE, although there is a wide spread of orientations due to their curvilinear planform geometry (Fig. 4). Plumose features, observed on the margins of sills where they step through stratigraphy, form fan-like features with parallel striae down their centre and diverging striae away from the central axis (Fig. 4c). The direction of striae divergence is to the S, with a range from SW-SE. The dykes maintain a constant thickness at the scale of the outcrop, and are orientated N-S to NNE-SSW (Figs 3b and 4b).

Interpretation

All injectites studied in this area are close to the base of Fan 3 (Figs 3a and 4a), with sub-vertical dykes connecting Fan 3 with the large stepped sill. In the SE part of the outcrop, dykes directly connect the parent sand to the sill (Fig. 3), which supports local downward propagation (e.g. Von Brunn & Talbot, 1986; Rowe *et al.*, 2002; Parize & Friès, 2003; Le Heron & Etienne, 2005). The fine sand grain-size of the injectites is the same as Fan 3, and Fans 1 and 2 are not present in the underlying stratigraphy, which comprises several 100′s m of mudstone (King *et al.*, 2009). Consequently, Fan 3 is interpreted as the parent sand for all the injectites.

The dykes are orientated approximately perpendicular to the NW-facing palaeoslope that confines Fan 3. Therefore the dyke orientation is hypothesized to relate to a gravitational stress regime. Although the injectites occur beneath the parent sand, the morphology of the curved steps and the orientation of structures on the injectite surfaces (Fig. 4b) (plumose features indicate the propagation direction, Cobain *et al.*, 2015) suggest that the main injectite sill stepped laterally outwards from its centre and cut up stratigraphy towards the south and east. The injectites, therefore, parallel the base of Fan 3 and continue beyond the depositional pinchout (Figs 3a and 4a). Net injection propagation direction was horizontal rather than vertical from the sharp-based sandbody with an abrupt upslope pinchout configuration in a lower slope to base-of-slope setting.

Zoutkloof; Laingsburg depocentre

Unit architecture

Unit C of the Fort Brown Formation (Fig. 1b) has also been the focus of extensive study, and is subdivided into three subunits; C1, C2 and C3, each separated by a laterally extensive mudstone (Di Celma *et al.*, 2011; Flint *et al.*, 2011; Hodgson *et al.*, 2011a; van der Merwe *et al.*, 2014). Extensive dip and strike outcrop control allow the distribution of sedimentary facies and architectural elements, and therefore depositional environments, to be constrained (Di Celma *et al.*, 2011). Subunit C1 forms a 50 m thick lobe complex 8 km to the southeast (Fig. 5) where the overlying subunit C2 is thin-bedded and forms part of an external levee to a channel system (Di Celma *et al.*, 2011; van der Merwe *et al.*, 2014). At the Zoutkloof locality, subunit C1 is sharp-based, thins from 2 m of amalgamated fine sandstone (Fig. 6c) to <12 cm thin bedded very fine sandstone over ~1.5 km at the oblique up dip pinchout of the lobe complex (Fig. 6b). The confining palaeoslope at subunit C1 time, based on isopach thickness maps and palaeocurrents, was orientated N-S and E-facing (Di Celma *et al.*, 2011; Fig. 5). Locally, the base of C1 forms a sharp contact with the underlying mudstone, and the top surface is marked by the lower C mudstone that

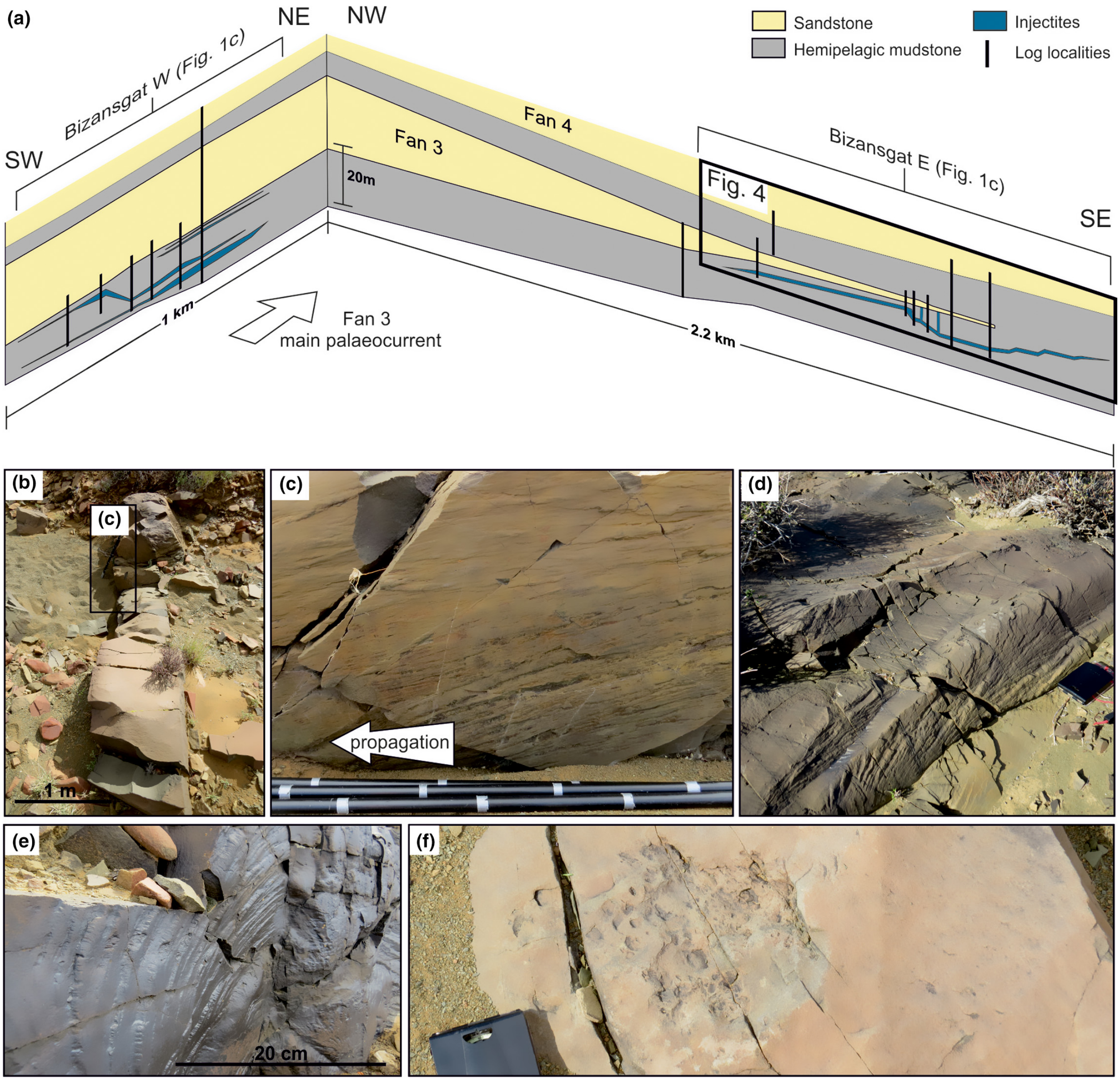

Fig. 3. Bizansgat outcrop – correlation panels and injectite margin structures. (a) Correlation panel of logs taken at Bizansgat through Fan 3 and injectites. (b) Typical dyke connecting base of Fan 3 with sheet sill displayed in (Fig. 4b). (c) Ridges on margin of dyke indicating injectite propagation direction. (d) Example of plumose pattern on the fracture surface along the top margin of small-scale step. (e) Plumose pattern on a fracture surface along sill step. (f) Patch of mudstone clasts on top surface of a sill.

separates subunits C1 and C2 (Di Celma *et al.*, 2011) at a constant thickness of 0.9 m. This upper mudstone was used as a datum (Fig. 6a and d).

Zoutkloof injectites

At Zoutkloof, injectites crop out over 1.7 km (Fig. 6d–f) below subunit C1, in the upper 13 m of the 40 m thick regional mudstone that separates Units B and C (Brunt *et al.*, 2013), at an abrupt, oblique lateral pinchout (Di Celma *et al.*, 2011) (Figs 5 and 6d). At this locality, the main form of injection is stepped sills (Fig. 6f). Curved steps are no more than 2 m in vertical height and continue laterally for 10's m. Steps are closely spaced so that the sills are discordant with the host stratigraphy for more than 2–3 m. The majority of dyke margins exhibit ridges, both plumose and parallel (Cobain *et al.*, 2015). Several sub-vertical dykes are observed to connect the base of subunit C1 with the stepped sills, the thickest is 1.5 m wide (between logs 7 and 8; Fig. 6a). Most other dykes are thinner (<0.3 m-thick) and connect with the base of subunit C1.

The steps and parallel ridges are primarily aligned E-W and the orientation of striae divergence of plumose patterns on the fracture surfaces is dominantly WSW (Fig. 6d). The dominant trend in dyke orientation measurements is NNW-SSE, approximately perpendicular to the orientation of the steps (Fig. 6).

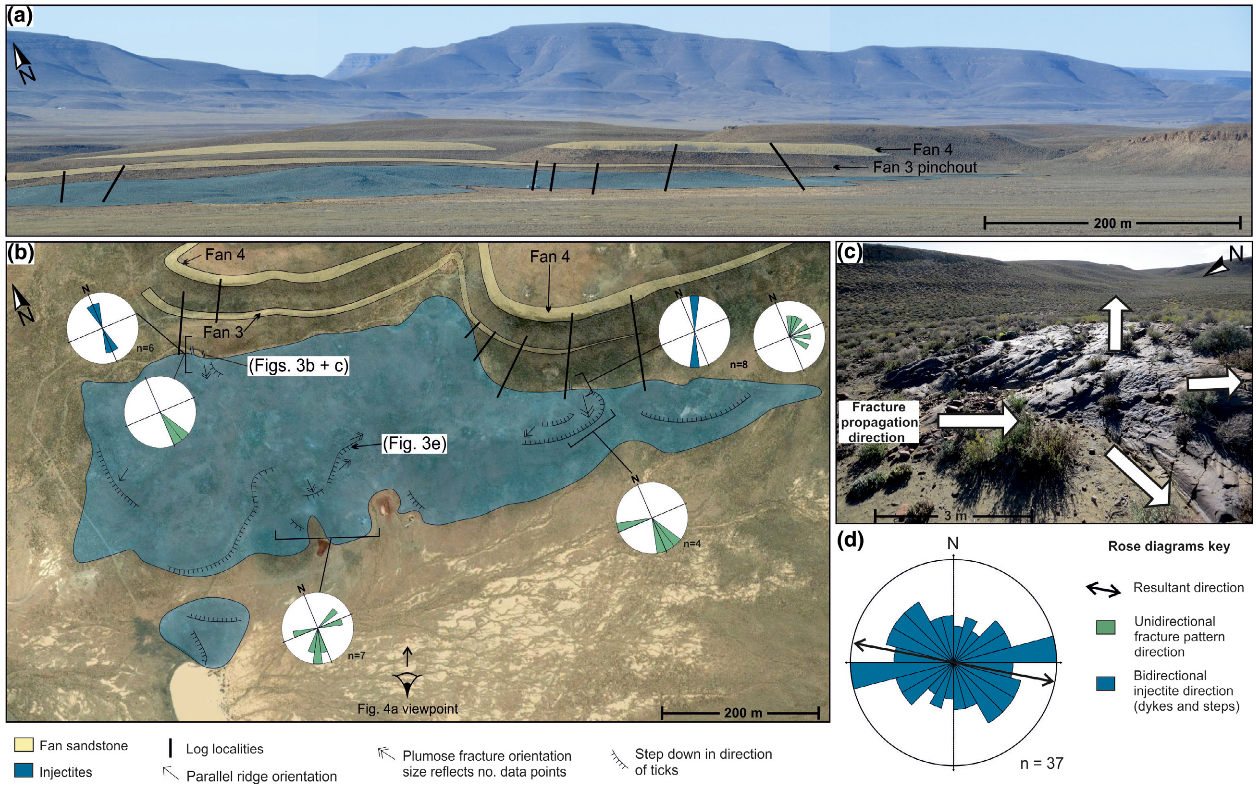

Fig. 4. Bizansgat outcrop – injectite geometries and orientations. (a) Panel view of outcrop showing extent of injected sandstone beyond that of the parent sand. (b) Map view of study area, Fan 3 and Fan 4 outcrop shown stratigraphically above injected sands. Rose diagrams display orientation data for dyke orientation and patterns on a fracture surface. (c) Photograph depicting large plumose fracture, main propagation direction is SE with diverging striae spanning almost 180°. (d) Rose diagram of step orientation across entire outcrop, widespread variation in direction due to curvilinear nature of steps but prominent step direction is E-W.

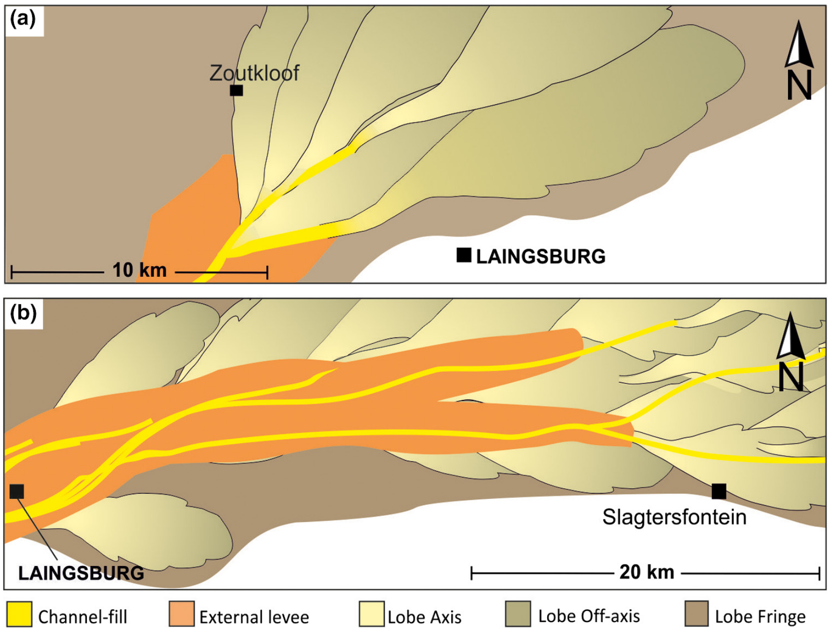

Fig. 5. (a) Palaeogeography of subunit C1, clastic injectites are present at Zoutkloof locality. (b) Palaeogeography of subunit C2, injectites are present along outcrop at Slagtersfontein (van der Merwe *et al.*, 2014).

Interpretation

In the Zoutkloof area, all injectites are close to the base of subunit C1, at the NW margin of the sharp-based lobe complex, and vertical dykes connect large stepped sills with the base of subunit C1. Therefore, subunit C1 is interpreted to be the parent sand of the injectites. The main sills, fed by dykes sourced from the overlying parent sand, abruptly step up stratigraphy to parallel the abrupt pinchout of the parent sand. Injection propagation is subparallel (WSW) to the unit pinchout direction and occurs where the base of parent sand has a sharp sand-to-mud contact. The orientation of the dykes is close to perpendicular to the slope-facing direction suggesting a causal relationship. The apparent propagation direction of subvertical dykes is downward but the ridges on the dyke margins suggest that propagation during injection was dominantly lateral (e.g. Kane, 2010).

Slagtersfontein; Laingsburg depocentre

Unit architecture

C2 is the only subunit of Unit C present in the Slagtersfontein region of the depocentre. The tabular sandstones with intercalated hybrid beds support palaeogeographic and isopach maps that indicate the location to be at the edge of a lobe complex that thins abruptly to the south (Fig. 5), with palaeoflow towards the east (van der Merwe *et al.*, 2014). These data suggest a WNW-ESE trending and NNE-facing confining palaeoslope during deposition of subunit C2 at Slagtersfontein (van der Merwe *et al.*, 2014). The top of the underlying Unit B consists of a widespread thin-bedded siltstone succession. The base of the overlying Unit D comprises tabular structureless sandstones (van der Merwe *et al.*, 2014; Hodgson *et al.*, 2016), therefore this was chosen as a datum from which to hang the panel (Fig. 7a). Along the Slagtersfontein outcrop, subunit C2 is sand-prone, sharp-based, and thickens from 0 m at the western extent of the outcrop to >20 m thick downdip to the east over 1.5 km. Lower beds within subunit C2 are structureless and amalgamated sandstones, whereas the upper beds are thin bedded and laminated (Fig. 7b). Locally, the base of subunit C2 is erosional, and incises underlying mudstones to the east (e.g. Fig. 7b).

Slagtersfontein injectites

Injectites exposed in the Slagtersfontein area are hosted within the regional mudstone separating Units B and C. The majority of injectites at the Slagtersfontein outcrop are 0.1–0.6 m thick sills that extend laterally for up to 500 m. Dykes (0.1–0.5 m thick) are common near the base of subunit C2, and are observed to connect to the base of Unit C (Fig. 7b and c). Injectites crop out over the entire exposure length of Unit C, and for a further kilometre up dip where Unit C is absent in the mudstone separating Units B and D (Fig. 7a). Injectites in the mudstone that separates Units B and C are most abundant close to, and directly connect with, Unit C where the base is erosive and has a sharp contact between the Unit C sandstone and the underlying mudstone. Injectite margins are mostly planar, although some parallel ridges are present on dykes. Some smaller injectites, mainly <0.2 m thick sills, occur close to the base of, and are directly connected to, Unit D (Fig. 7a). The outcrop character at Slagtersfontein only permitted collection of dyke orientation data, the mean of which is NW-SE (Fig. 7).

Interpretation

Injectites connect directly with subunit C2, therefore this is interpreted to be the parent sandstone for the main injectite network, with Unit D likely acting as a minor source (see Fig. 7a; direct connection of 2 small dykes between logs 9 and 10). The underlying Unit B is topped with several metres of thin bedded silty strata, which is consequently less likely to produce sandstone injectites; there is also an absence of any dykes emanating from this unit, in outcrop. The parent sand is at an abrupt sand-prone pinchout of a lobe complex (subunit C2) where locally the base is in erosive contact with underlying mudstones. The majority of clastic injectites are sills that extend laterally beyond the parent sand towards the west in cross-section (Fig. 7a). Therefore, the net propagation direction of injected sand was to the west and south, with injectites exploiting pre-existing bedding plane weaknesses (Cobain *et al.*, 2015). The orientation of the dykes are sub-parallel to the local NNE-facing palaeoslope, which suggests a causal relationship, such as a gravity-driven stress regime.

Comparison of study areas

Previous research in the Karoo Basin (Wickens, 1994; Wickens & Bouma, 2000; Hodgson *et al.*, 2006; Oliveira *et al.*, 2009; Prélat *et al.*, 2009; Di Celma *et al.*, 2011; Flint *et al.*, 2011; Brunt *et al.*, 2013; van der Merwe *et al.*, 2014) means that the palaeogeographic context of the parent sandbodies to the studied injectite networks is extremely well constrained. The style and extent of outcrop means that it has been possible to collect data and geometries of injectite networks to provide 3D constraints over several kilometres. The Fan 3 and Unit C study sites were deposited in basin-floor environments (Hodgson *et al.*, 2006; Di Celma *et al.*, 2011; Brunt *et al.*, 2013). Injectites sourced from Fan 3 in the Tanqua area, and subunits C1 and C2 in the Laingsburg area, coincide with sites of abrupt basin-floor sand-prone pinchout, with mudstone above and below. Additionally, the basal contact of the parent sand with the underlying mud is erosional and/or sharp where injection occurs. The injectites propagated laterally paralleling the base of the parent sandbody, and extend beyond the pinchout, and dykes are sub-parallel to the strike of the palaeoslope in all examples. Furthermore, the extensive previous research in the field area also helps to constrain where injectites are not present, meaning models are not biased towards outcrops that only show injectites. For example, detailed mapping and coring of the fringes of lobe complexes (Johnson *et al.*, 2001; van der Werff & Johnson, 2003; Hodgson *et al.*, 2006; Prélat *et al.*, 2009) has identified only rare isolated injectites associated with Fan 1 and Fan 4.

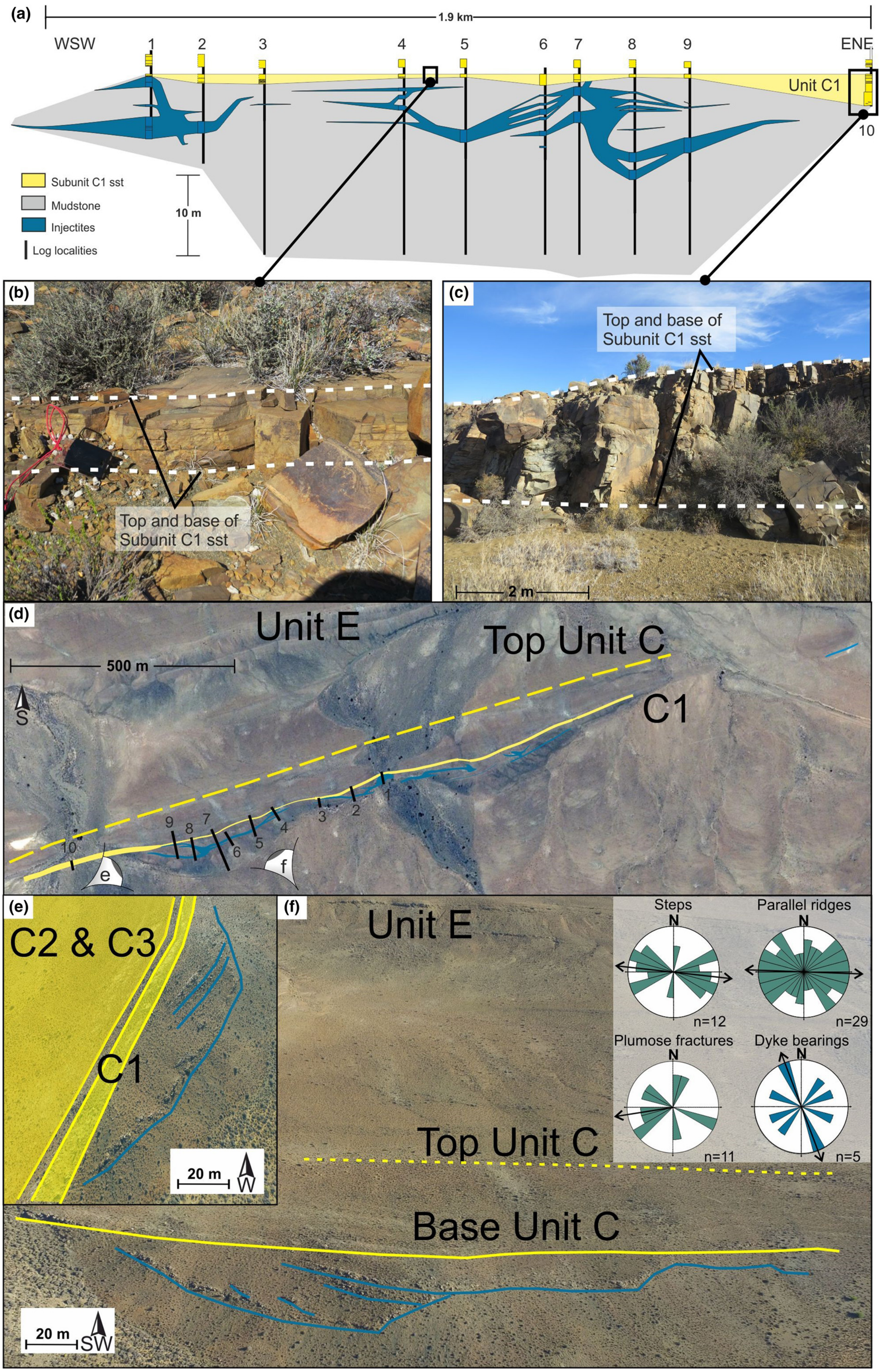
(a)
1.9 km
WSW
1
2
3
4
5
6
7
8
9
ENE
Unit C1
10
Subunit C1 sst
Mudstone
Injectites
Log localities
10 m
(b)
Top and base of Subunit C1 sst
(c)
Top and base of Subunit C1 sst
2 m
(d)
Unit E
Top Unit C
500 m
S
C1
e
f
(e)
C2 & C3
C1
20 m
W
(f)
Unit E
Steps
Parallel ridges
N
n=12
n=29
Plumose fractures
Dyke bearings
n=11
n=5
Top Unit C
Base Unit C
20 m
SW

Fig. 6. Zoutkloof outcrop and injectites. (a) Correlation panel of logs taken along length of outcrop (see Fig. 6d for location). (b) Subunit C1 is a 10 cm thick very fine sandstone. (c) Subunit C1 is >2 m thick, massive, fine sandstone. (d) Map view of outcrop with Subunit C1 highlighted, injectites and log locations indicated. (e) Oblique view, Unmanned Aerial Vehicle (UAV) based, photograph of clastic dykes and sills at eastern end of Zoutkloof exposure (see Fig. 6d for viewing direction). Subunit C1 is highlighted. (f) UAV photograph of Zoutkloof area showing the bowl-like structure of the injectite complex at the eastern end of the exposure (see Fig. 6d for viewing direction). Rose diagrams depict directional data for patterns on a fracture surface and step and dyke orientations. Refer to Fig. 4 for rose diagram colours.

DISCUSSION

Injectite emplacement in the Karoo Basin: mechanisms and controls

We have presented three examples of basin-floor lobe complex pinchouts that have been subject to post-depositional fluidization of the parent sandbody and clastic injection into the surrounding mudstone. Discussion on emplacement takes into account the common features observed across all outcrop examples described here, the well-constrained architecture and palaeogeography of each of the units, and the prerequisite conditions needed for clastic injection.

Conditions prior to injection

Typically, the same conditions observed to form overpressured and uncemented sand liable to fluidization in slope channel-fills are also met in these examples from basin-floor lobe complexes: (i) proximal deposits within the lobe complexes provide clean, fine to very fine sand (e.g. Marchand *et al.*, 2015) that increases the likelihood of fluidization, and hence susceptibility for sediment transport (Richardson, 1971; Jolly & Lonergan, 2002); and (ii) the deep-marine environment and regional changes in clastic sediment supply allow for alternating sand-rich channel-fed lobe complexes encased by regional hemipelagic mudstone drapes that provide the seal required for overpressure to develop (Lorenz *et al.*, 1991; Cosgrove, 2001; Jolly & Lonergan, 2002). These surrounding mudstones may also provide an additional source of pore fluids during the initial stages of compaction (Magara, 1981).

Geographic location and parent sandstone architecture

Based on the outcrop positions of the observed injectites, and the existing palaeogeographic knowledge of the Karoo Basin (Wickens, 1994; Wickens & Bouma, 2000; Hodgson *et al.*, 2006; Oliveira *et al.*, 2009; Prélat *et al.*, 2009; Di Celma *et al.*, 2011; Flint *et al.*, 2011; Brunt *et al.*, 2013; van der Merwe *et al.*, 2014; Hofstra *et al.*, 2017), the injectites are interpreted to be located at the abrupt pinch-out of sand-rich lobe complexes (Figs 3 and 5). At their abrupt updip pinchout, such as Bizansgat (Fan 3) and Zoutkloof (subunit C1) the parent sand is generally homogenous, well-sorted, and has a sharp contact with the underlying strata. The same configuration occurs in the abrupt lateral pinchout at Slagtersfontein (subunit C2). Clastic injectites occur stratigraphically beneath the parent sandstone, with net lateral propagation towards and beyond the margin of the parent sandstone lobe complex. In other examples, where injectites of seismic-scale are known to be sourced from lobe complexes (as observed in intra-slope lobes), the source point is the proximal lobe (complex) fringe (Yang & Kim, 2014; Spychala *et al.*, 2015), or the lateral lobe margin pinchout (Monnier *et al.*, 2014). In the latter case, the lobe reaches its highest point laterally. This suggests that an abrupt and sand-prone pinchout in the most elevated position on the lobe, which will typically occur in the proximal or lateral parts of lobes, is a preferential site for clastic injection processes.

Nature of stratigraphic contact

Considering the geographic and stratigraphic distribution of the required unconsolidated sandstone and the surrounding fine grained sediments, injectites might be expected at all positions within lobe complexes. As long as sand remains unconsolidated, the surrounding hemipelagic mud may form a seal around the entire unit. The observation of preferential hydraulic fracture at a sharp sand-to-mud contact, with clean sands, however, favours the proximal area of lobe complexes at their base. In these situations, erosional relationships and/or steeper slopes promote a more abrupt onlap geometry and the formation of a sharp basal contact from where the injectites are sourced. Commonly, the upper part of lobe complexes are thin-bedded (e.g. Hodgson *et al.*, 2006; Prélat *et al.*, 2009), and in such cases injectites are absent. In the presence of subtle confinement (Sixsmith *et al.*, 2004), or in more distal settings (van der Werff & Johnson, 2003; Hodgson, 2009; Prélat *et al.*, 2009; Spychala *et al.*, 2017), injectites are not observed. However, in a few cases where there is an abrupt sand-to-mud contact on top of a lobe complex, due to large-scale avulsion or sudden clastic input shutdown, injectites are observed (e.g. Subunit A5; Cobain *et al.*, 2015). Where clastic material is finer and/or less well-sorted, clastic injection is not observed. What mechanism controls this preferential occurrence of injectites at the interface between clean sands and muds? A key attribute of clean sands is a tighter grain-size and shape distribution, and therefore higher permeability relative to less clean sands (Krumbein & Monk, 1942; Beard & Weyl,

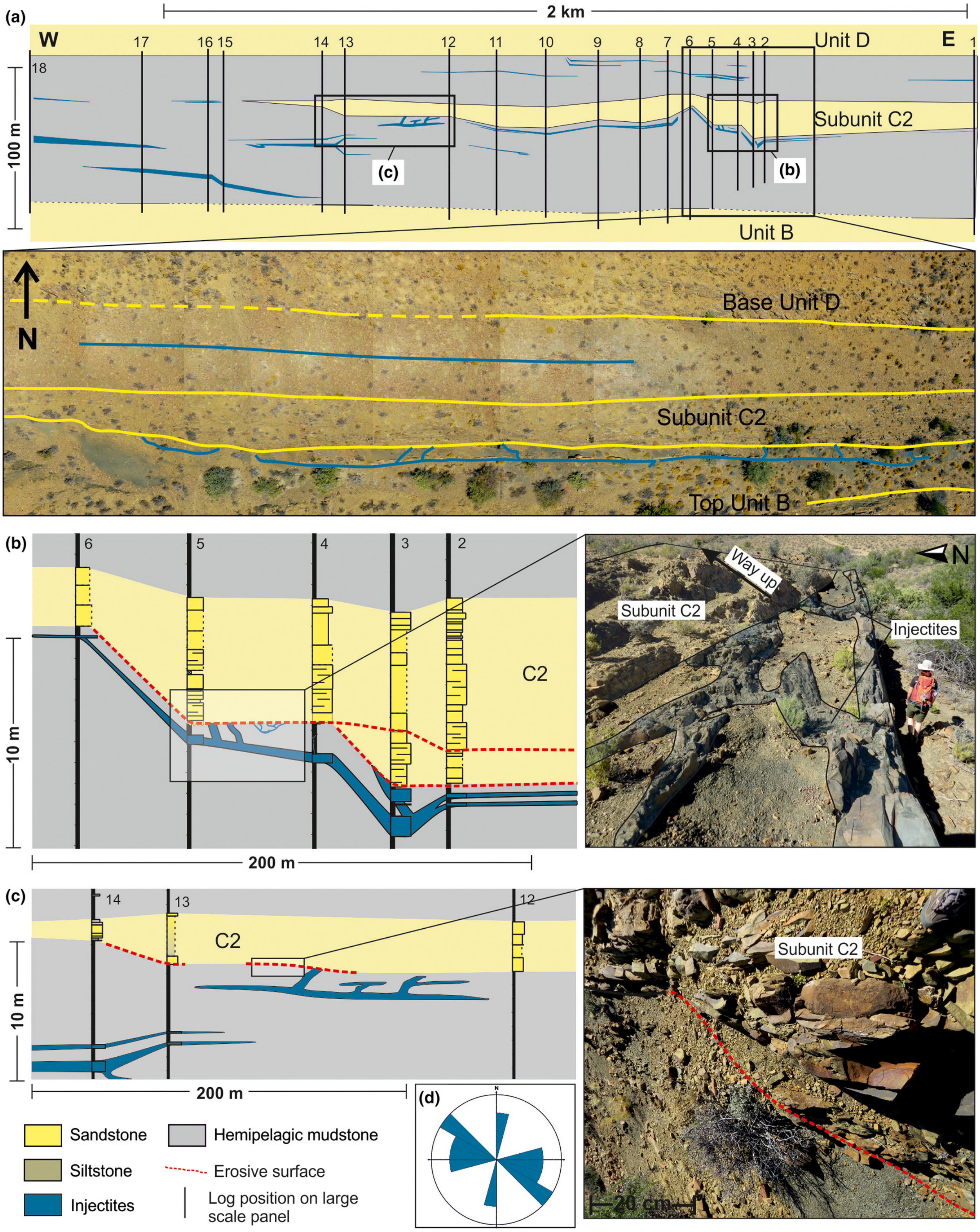

Fig. 7. Slagtersfontein outcrop and injectites. (a) Correlation panel of logs (numbered) through Unit C2, injectites present throughout (C2 is the only subunit of Unit C to be present). Inset of UAV based photograph highlighting Subunit C2 and clastic dykes and sills. (b) Section through logs 2-6, where C2 has an erosive base, and dykes directly connect with the base of C2. Inset shows expression of unit and injectites at outcrop. (c) Section through logs 12-14, where a single dyke extends from the base of C2 and feeds the sill/dyke network. Inset depicts example of erosive base. (d) Rose diagram displaying orientation of dykes below Unit C, these are oblique-strike to the likely palaeoslope, which locally was NNE-facing based on the isopach maps of van der Merwe *et al.* (2014).

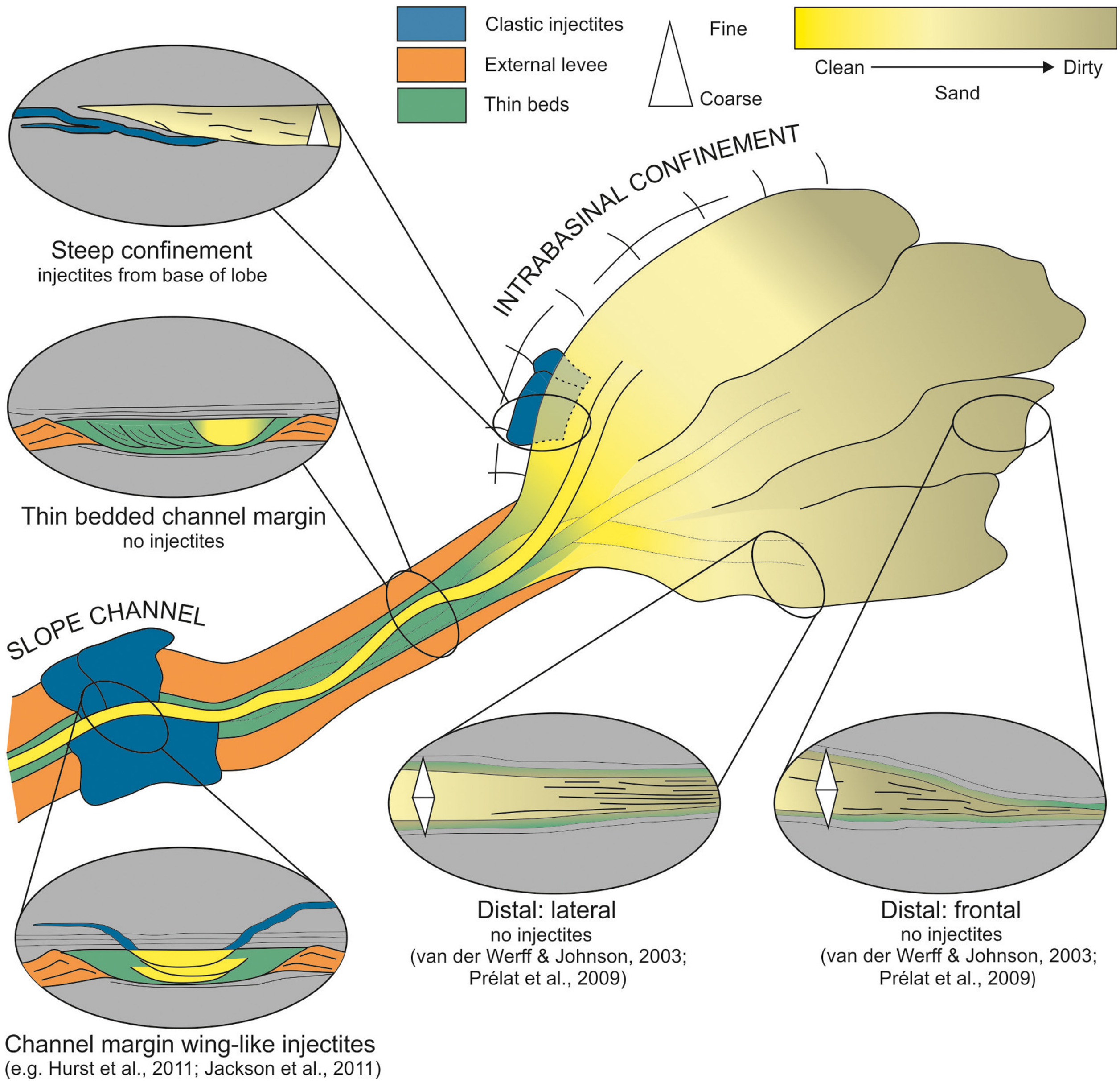

Fig. 8. Schematic diagram to indicate likely areas of injection in a deep marine system; examples of previously reported clastic injectites occur on the slope (Huuse *et al.*, 2004; Jackson *et al.*, 2011) (note that injectites in this setting may be more broad ranging), whereas this study reports examples from basin-floor lobe complexes. Injectites occur in areas where sand is steeply confined and/or proximal within the lobe complex, while palaeogeographic locations that are downdip exhibit subtle confinement or have less clean-sand for fluidization and therefore do not produce injectites.

1973). Transient changes in pressures related to variations in grain-size, and thus permeability, might be expected to influence the position of hydraulic fracturing. However, cyclic loading of sands in closed systems demonstrates that lower permeability sands exhibit higher transient pressures (e.g., Kelly *et al.*, 2006). Consequently, variations in permeability do not appear to be the controlling mechanism. Furthermore, if aseismic, overpressure builds more gradually over geological time, and therefore the pressure at the sand-mud boundary may be similar at all points. In contrast, clean sands are more susceptible to fluidization (Richardson, 1971; Jolly & Lonergan, 2002), and consequently they may preferentially fill any hydraulic fractures that occur.

Possible trigger mechanisms

In order to develop the overpressure required to fluidize and liquefy parent sand, and subsequently inject it into the surrounding strata, a trigger mechanism is required (Jolly & Lonergan, 2002; Oliveira *et al.*, 2009). Several different trigger mechanisms have been postulated to account for clastic injectites in deep-marine environments: seismicity (e.g. Obermeier, 1996; Boehm &

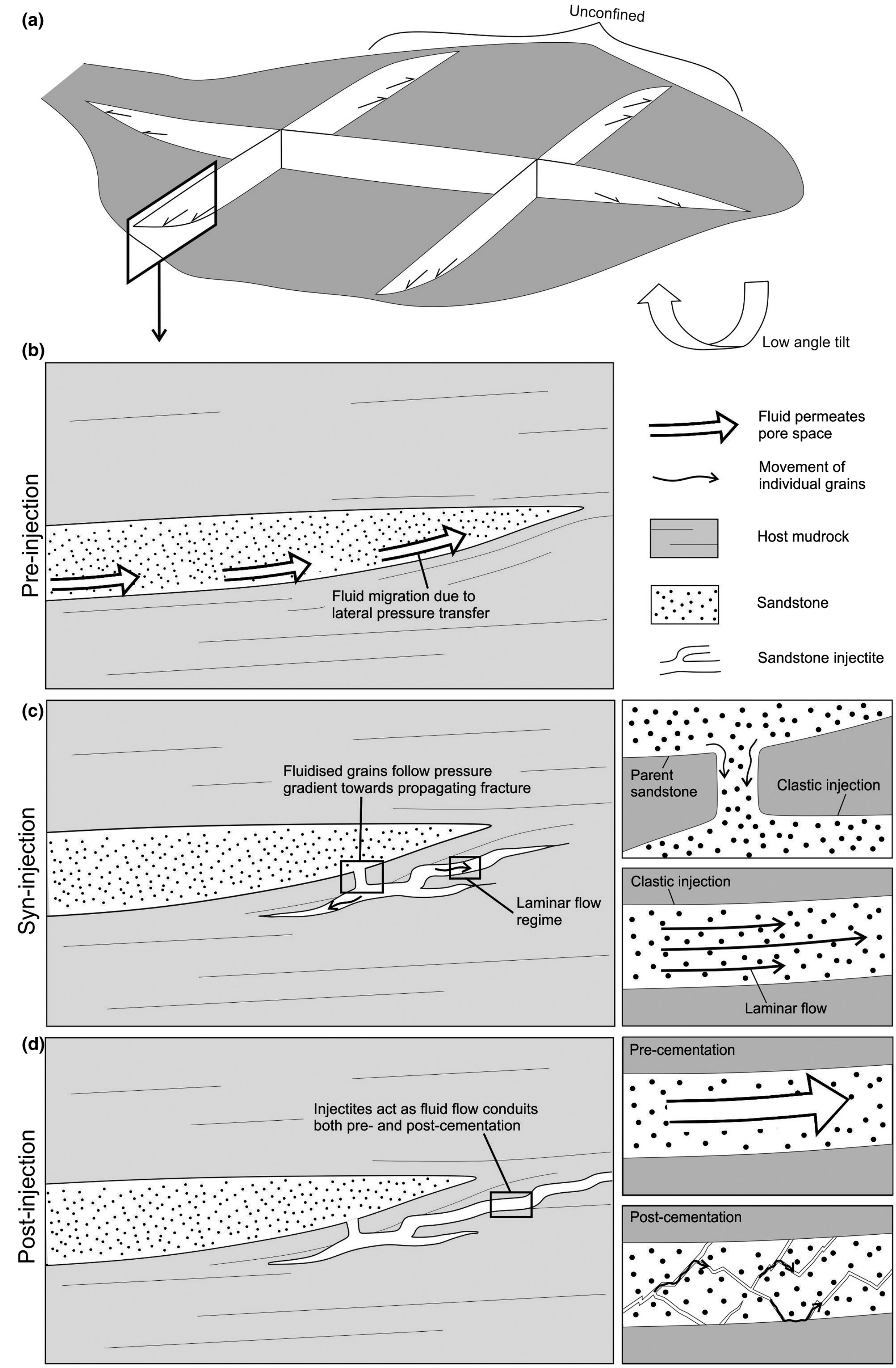

(a)
Unconfined
Low angle tilt
(b)
Pre-injection
Fluid migration due to lateral pressure transfer
Fluid permeates pore space
Movement of individual grains
Host mudrock
Sandstone
Sandstone injectite
(c)
Syn-injection
Fluidised grains follow pressure gradient towards propagating fracture
Laminar flow regime
Parent sandstone
Clastic injection
Clastic injection
Laminar flow
(d)
Post-injection
Injectites act as fluid flow conduits both pre- and post-cementation
Pre-cementation
Post-cementation

Fig. 9. Fluid flow associated with stages of clastic injection. (a) Simple lobe complex architecture, injectites sourced from steeply confined margin. (b) Overpressured sandstone: pre-injection overpressure from compaction and expulsion of fluids from surrounding strata followed by fluid flow due to lateral pressure transfer. (c) Trigger and fluidization: syn-injection fluid flow, grains liquefied and fluidized into propagating fracture. d) Diagenesis: post-injection fluid flow, both pre- and post-cementation.

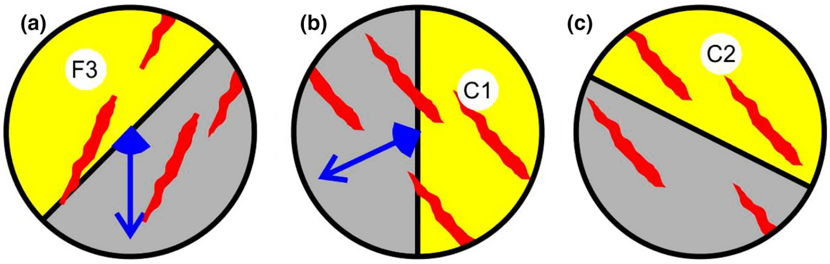

Fig. 10. Simplified map view illustrations of the orientation of parent sand pinchout and injectites at the three study sites, (a) Bizansgat (Fan 3), (b) Zoutkloof (subunit C1) and (c) Slagtersfontein (subunit C2). The yellow marks the parent sand, the grey is the underlying mudstone. The red lines are dykes, using mean orientation. The blue arrows show the mean direction for flow of the intrusions where recorded. Note that the dykes are sub-parallel to the pinchout of the sandbody (approximately perpendicular to the onlap slope) and that the dominant flow direction is at a high angle to the pinchout.

Moore, 2002; Huuse & Mickelson, 2004; Obermeier *et al.*, 2005), tectonic stress (e.g. Peterson, 1966; Jolly & Lonergan, 2002), rapid burial (e.g. Truswell, 1972; Allen, 2001), instability of overlying sediments (e.g. Hiscott, 1979; Jonk, 2010) or migration of basinal fluids into the sealed sand body (e.g. Vigorito & Hurst, 2010; Jackson *et al.*, 2011; Bureau *et al.*, 2014; Monnier *et al.*, 2014).

A substantial depth of burial prior to sand injection in the Karoo Basin examples examined herein consists of a number of lines of evidence, including the preservation of initial brittle, hydraulic patterns on fracture surfaces on the margins of injectites seen at the Zoutkloof and Bizansgat localities (Fig. 3d and e). These suggest that the muds were sufficiently hard to form and maintain these surface patterns; no evidence for later compaction of these surface patterns on dyke margins is observed (Cobain *et al.*, 2015). Furthermore, the observed injectites show features (vertical distribution of particles within sills; lack of erosion) commensurate with high-concentration, laminar flow conditions, suggesting that the units were sufficiently far from the contemporaneous seabed that breakthrough and subsequent extrusion did not occur; such open-conduit conditions are linked to turbulent flow conditions (Cobain *et al.*, 2015). However, despite the evidence given above that injection did not occur at very shallow depths, the fact that the injection occurred along extensional fractures, places a constraint on the depth at which they formed. The conditions for the formation of extensional fracture is that the differential stress should be less than 4 times the tensile strength (T) of the rock, (i.e. $(\sigma 1-\sigma 3) < 4T$), (see e.g. Cosgrove, 2001). The differential stress increases with depths and extensional fractures can only form above the depth where $(\sigma 1-\sigma 3) = 4T$. It is suggested that in the study area this depth was around several hundred metres. There is a notable absence of overlying slides and slumps, and the absence of growth strata above seabed folds and faults in the basin-fill (e.g. Hodgson *et al.*, 2006; Di Celma *et al.*, 2011; Flint *et al.*, 2011; Jones *et al.*, 2015) indicate it was largely tectonically quiescent. Therefore, fluidization and injection due to localized excess pore fluid pressures generated by depositional processes such as mass flows (Truswell, 1972; Jolly & Lonergan, 2002) and shallow seismicity (Obermeier, 1996; Lunina & Gladkov, 2015), in these outcrop examples, are considered unlikely trigger mechanisms.

Disequilibrium compaction is a major source of overpressure in sedimentary basins (Osborne & Swarbrick, 1997), however within a single body or unit, this overpressure will dissipate over geological time, and high overpressures can only be maintained in the shallow subsurface through high rates of sedimentation (Jonk, 2010). Therefore, disequilibrium compaction alone may not be an adequate source of overpressure to trigger clastic injectites. Overpressure due to fluid volume increase is associated with aquathermal expansion and clay dehydration, though these alone are considered too insignificant to generate high amounts of overpressure (Osborne & Swarbrick, 1997). Deep or regional seismicity has been commonly cited as a primary cause of sand intrusion, however, the energy required to fluidize and inject such quantities of sand in regionally extensive injectites likely exceeds that produced by earthquakes (Huuse *et al.*, 2005; Duranti, 2007; Vigorito & Hurst, 2010). If such regional seismicity were a cause, then hydraulic fracturing, failure of encasing mudstone, and resultant injection would be expected across the entire lobe complex. Additionally, an absence of seismicity for a significant period would be needed in order to bury the sediments to depth and enable overpressure to build; consequently, a large-scale change in tectonic regime would be required.

Regional seismicity, therefore, is considered an unlikely trigger of injection for these deeper injectites (Duranti, 2007; Hurst *et al.*, 2011).

Another mechanism for triggering injection in deep-water systems is the migration of fluids caused by lateral pressure transfer: the lateral transfer of fluids from deeper, overpressured parts of the basin along laterally extensive, inclined, porous units (Osborne & Swarbrick, 1997; Yardley & Swarbrick, 2000). The lower parts of the basin-fill are likely to experience enhanced overpressure as a result of compaction, and thus cause movement of fluid upwards towards the highest point. This form of fluid migration is most likely to be concentrated at the up dip margins of a unit (Cartwright, 2010), such as a lobe complex margin, where the abrupt pinchout architecture at the fringe of lobe complexes promotes fluid migration towards the edge (Monnier *et al.*, 2014). The surrounding mud limits further fluid migration. Migration of fluids due to lateral pressure transfer operates in basins such as the Gulf of Mexico, where simple tilting causes a pressure gradient (Flemings *et al.*, 2002; Gay *et al.*, 2011). Lateral pressure transfer is interpreted to be the likely cause of post-Eocene intrusions along the margin of the San Joaquin Basin (Schwartz *et al.*, 2003; Cartwright, 2010). In the San Joaquin Basin, the fluids that produce overpressure and cause lateral pressure transfer are not derived locally. Migrating hydrocarbons may also cause an increased pore pressure in sand units sealed by impermeable strata (Jolly & Lonergan, 2002). Consequently, increased overpressure of an unconsolidated sand body by compaction driven fluid expulsion, and fluid migration through lateral pressure transfer (water, oil, gas), is the preferred trigger mechanism responsible for clastic injection in the Karoo Basin (see also Cobain *et al.*, 2015). The parent sand architecture in all examples promotes lateral fluid migration to the updip lobe complex margins. Larger-scale injectites have also been attributed to this kind of trigger (Huuse *et al.*, 2005; Hurst *et al.*, 2011; Løseth *et al.*, 2013).

An integrated model of injectites in basin-floor lobes

Synthesizing the observations discussed previously enables an integrated model of injectites in basin-floor lobes to be proposed. Injectites are observed to form preferentially at the updip margins of basin-floor lobe complexes (Bizansgat Fan 3 and Zoutkloof subunit C1) and on lateral margins where the pinchout is abrupt and sand-prone (Slagtersfontein subunit C2) (Fig. 8). This geographic distribution is linked to the nature of the triggering mechanisms. The presence of patterns on fracture surfaces, the absence of significant compaction of these structures, and the evidence for confined laminar flow, suggest that these injectites formed at substantial depths, but the extensional nature of fracturing indicates a maximum depth of no more than a few hundred metres. Consequently, disequilibrium compaction and lateral pressure transfer are the likely trigger mechanisms, and in the case of a lobe complex deposited above a basinal slope, these mechanisms will lead to updip fluid migration. Furthermore, in a tilted sandbody the confining lithostatic pressure will also decrease updip. Therefore, hydraulic fracturing will predominantly occur at the up-dip margin where fluid migration and the lowest confining pressures combine. Within the proximal lobe complex, injectites are shown to occur at pinchouts (Figs 8 and 9); these areas both concentrate fluid-flow from lateral transfer and provide sharp boundaries at their basal surfaces between clean sands and the underlying mudstones. We argue that initiation of hydraulic fracturing is favoured at the bases of these pinchouts because these clean sands are the most susceptible to fluidization (Richardson, 1971; Jolly & Lonergan, 2002) and therefore will preferentially infill any hydraulic fractures that occur. Theoretically, hydraulic fracturing might be expected to occur on the upper surface of the most up-dip point, as shown in some examples (Cobain *et al.*, 2015), but in many cases proximal parts of lobes exhibit a transition towards lower permeability facies (e.g., thinner bedded siltstones and sandstones) at their tops (Fig. 8; Prélat *et al.*, 2009). The distal parts of basin-floor lobes are not favoured sites for injection as a consequence of their down-dip position, and their more heterogeneous, mud-rich, facies including thin-bedded silts and sands, and hybrid beds (Fig. 8; Hodgson, 2009; Prélat *et al.*, 2009; Marchand *et al.*, 2015; Spychala *et al.,* 2017). Whilst the physical linkage between sills and the parent sands suggests that the initial hydraulic fracturing and injection can be downwards, the increasing lithostatic pressure below the parent sands will encourage lateral propagation with sands able to step beyond the lobe complex margins (Figs 8 and 9). This is supported by the direction of injection flow being at a high angle to the orientation of sand pinchout (Fig. 10).

The dykes at all three study sites are aligned sub-parallel to the strike of the palaeoslope (Fig. 10), which suggests that a controlling factor in injectite morphology is the orientation of the slope onto which the lobes onlap. Tensile features would preferentially develop perpendicular to slope facing direction in a gravitational stress field, leading to a narrow range of dyke orientations after injection was triggered. This would provide the necessary anisotropy for the documented preferred direction. In contrast, several studies have found limited to no relationship between injectite orientation and palaeoslope (Hiscott, 1979; Rowe *et al.*, 2002; Diggs, 2007; Jackson, 2007; Vétel & Cartwright, 2010; Bain & Hubbard, 2016; Palladino *et al.*, 2016), and ascribe measured orientations to later tectonic controls (e.g. Diggs, 2007; Vétel & Cartwright, 2010; Palladino *et al.*, 2016), or in association with submarine channel orientation (e.g. Jackson, 2007) and/or the emplacement direction of mass transport emplacement (Hiscott, 1979; Rowe *et al.*, 2002). However, here we demonstrate that for injectites sourced from lobe complexes in tectonically quiescent basins, palaeoslope can be a controlling factor on injectite orientations.

Stages of fluid flow associated with injectites

Understanding fluid flow through time in sedimentary basin-fills is essential when considering aquifers and hydrocarbon reservoirs. In large-scale cases, injectites can promote basin-wide fluid flow and offer vertical and lateral permeable networks through low permeability successions (Huuse *et al.*, 2005; Vigorito *et al.*, 2008; Jonk, 2010; Hurst *et al.*, 2011). Four main elements of basin-wide fluid flow are identified (Jonk *et al.*, 2005a): (i) gravity-driven, downward flow of meteoric water (Bjørlykke, 1993), (ii) compaction of sediments through burial causes fluids to be expulsed and flow upwards (Osborne & Swarbrick, 1997), (iii) upward flow of fluids through overpressure (Osborne & Swarbrick, 1997), and (iv) upward migration of hydrocarbons due to buoyancy (Bonham, 1980). Clastic injectites are associated with basinal fluid flow at several stages; pre-injection, during the process of clastic injection, post-injection and pre-cementation, and post-cementation (Fig. 9).

Pre-clastic injection

The migration of fluids as a trigger for clastic injectites through lateral pressure transfer has already been discussed; a schematic representation of the processes is shown in Fig. 9b.

During injection

During clastic injection, grains are suspended and transported down a pressure gradient, by fluids moving from the overpressured parent unit towards the tip of the propagating hydraulic fracture, a source of relatively lower pressure (Cosgrove, 2001). The flow regime during injection can be turbulent (Hubbard *et al.*, 2007; Scott *et al.*, 2009; Hurst *et al.*, 2011) or laminar (Duranti, 2007; Cobain *et al.*, 2015) (Fig. 9c).

Post-injection, pre-cementation

In previous studies, petroleum inclusions in late diagenetic cementation phases, and multiple cementation phases, indicate that injectites can act as long-lived fluid flow conduits (Jonk *et al.*, 2005b, c, 2007; Ross *et al.*, 2014). Injectites can act as fluid flow conduits up to depths of approximately 1 km (Jonk *et al.*, 2005a; Jonk, 2010) prior to cementation. However, thicker sandstones (i.e. 20–30 m) can remain uncemented up to depths of 1.5–2 km burial, for example those within the Tertiary of the Northern North Sea (Lonergan *et al.*, 2000; Duranti *et al.*, 2002). Additionally, many of the large-scale injectite networks in the Tertiary of the North Sea have maintained excellent reservoir properties (Hurst & Cartwright, 2007) and outcrop examples such as the Panoche Giant Injection Complex have been shown through fluid inclusion analysis to have maintained migration of fluid for almost 2 Ma post injection (Minisini & Schwartz, 2007; Hurst *et al.*, 2011). Besides acting as fluid migration pathways, clastic injectites can connect otherwise separate reservoirs, and form traps when injected solely into—or capped by—impermeable strata (Frey-Martínez *et al.*, 2007; Schwab *et al.*, 2015).

Post-cementation

When cemented, injectites become fluid flow barriers, preventing any further migration of basinal fluids. However, cemented injectites also have the potential to act as conduits, through structural deformation in the form of fractures focussed on the competent sands within low-competence mudrock host lithology (Jonk *et al.*, 2005a) (Fig. 9d). Understanding the timing of deformation phases helps to determine if clastic injectites will be reactivated as fluid flow conduits.

Implications for hydrocarbon extraction

Is there an association of stratigraphic traps and clastic injectites?

Each outcrop locality presented herein is an example of a basin-floor lobe complex that has been subject to clastic injection at its abrupt proximal (Bizansgat, Zoutkloof) or lateral (Slagtersfontein) pinchout. In each case, injectites are fed from the sharp sand-to-mud contact that marks the base of a lobe complex, they then parallel the base of the depositional body, stepping upwards and outwards (e.g. Figs 3a and 7a), ultimately projecting beyond the limit of the lobe complex. The clastic injectites produced are of sub-seismic scale.

Sandy lobe complexes such as those described have been a prime target for hydrocarbon exploration as stratigraphic traps (e.g., Halbouty, 1966; Walker, 1978; Brown *et al.*, 1995; Gardiner, 2006; Stoker *et al.*, 2006; Nagatomo & Archer, 2015). In particular, proximal turbidites on the basin floor as they provide clean sands that pinch out abruptly, providing an optimal trap configuration. We have shown that these sands are prone to injection, particularly on a sub-seismic scale. In addition, dykes can have a strong preferential orientation at abrupt pinchout of lobe complexes against confining slopes, and that injection flow will be towards, and beyond, sand pinchout. This helps to constrain the architecture and prediction of injectite networks at stratigraphic traps on the basin-floor. The presence of clastic injectites at stratigraphic traps can be beneficial; they can provide connection between otherwise separated sand units, allowing flow of hydrocarbons through impermeable mudrocks, and balancing pressure differences across reservoir complexes. However, the complicated geometry of injectites and their potential to connect otherwise separate sand bodies needs to be taken into consideration when building reservoir models and when using outcrops as analogues for geological and petrophysical model development.

Are basin-floor lobe injectites under-reported?

The relative lack of documented examples of injectites associated with lobe complexes compared to submarine slope channel-fills may simply be due to less of these systems being drilled and therefore a data bias. However, this disparity is also likely a reflection of scale. Parent sands of the injectites described here are volumetrically larger than many slope channel-fills, but comprise much thinner lobe complexes. Therefore, as observed in the Karoo Basin outcrops, thinner injectites can be expected as a product of remobilization in comparison to slope channel-fills, thus being sub-seismic scale and frequently unrecognized or poorly documented on many seismic data sets (e.g. Shepherd *et al.*, 1990). Another factor contributing to the lack of recognition in subsurface data is the style of injection; Karoo injectites are primarily laterally extensive sills. These would be hard to identify in reflection seismic data, and misinterpretation as primary deposits rather than remobilized units in core is possible.

CONCLUSIONS

The majority of injectites are reported as being sourced from channel-fills or intraslope lobes in submarine slope settings, and have been rarely documented in base-of-slope and basin-floor environments. The three outcrop examples of clastic injectites presented here are associated with basin-floor environments, and specifically occur at the abrupt pinchouts of basin-floor lobe complexes. Architecture and bed-scale similarities across the injectite parent sand have led to the development of a model to help predict likely areas and orientations of clastic injectites in a deep marine system. Injectites occur where sand is: (i) confined and pinches out abruptly, (ii) proximal within the lobe complex, and (iii) exhibits sharp contacts with underlying and/or overlying mudstone. In contrast, palaeogeographic locations that exhibit subtle to no confinement have less clean-sand for fluidization, and heterolithic stratigraphic boundaries do not result in injectites. Clastic injectites, even those of a sub-seismic scale, provide the potential to rearrange fluid flow pathways within deep-water successions. Injectites, such as those in the Karoo Basin, can extend laterally for several kilometres, and beyond the stratigraphic pinchout, yet are too thin to be resolved in seismic data. However they may connect otherwise separate bodies of sand or reservoirs, offering highly permeable networks through impermeable successions. The association of clastic injectites and stratigraphic traps can be beneficial in subsurface plays. This is because they provide connection between otherwise separate sand units, allowing flow of hydrocarbons through impermeable mudstones, and balancing pressure differences across reservoirs. In the Karoo Basin, we see clastic injection and therefore the potential for fluid flow in basin floor settings, where, up until now, injectites and associated fluid flow have dominantly been associated with channelized slope environments.

ACKNOWLEDGEMENTS

This research was funded by a Natural Environment Research Council PhD studentship (Ref. number NE/J016950/1) with Statoil as a CASE partner. The authors thank local landowners for their permissions to carry out fieldwork on their land and Colleen Kurcinka for her assistance in the field. We thank John Cosgrove, Aurelian Gay, and an anonymous reviewer, for detailed and perceptive reviews that have significantly improved the article. We also thank Editor Sébastien Castelltort.

CONFLICT OF INTEREST

No conflict of interest declared.

REFERENCES

Allen, J.R.L. (2001) *Principles of Physical Sedimentology: Reprint of First Edition (1985), With Corrections*, 272 pp. Blackburn Press, Caldwell.

Aydin, A. (2000) Fractures, faults, and hydrocarbon entrapment, migration and flow. *Mar. Petrol. Geol.*, **17**, 797–814.

Bain, H.A. & Hubbard, S.M. (2016) Stratigraphic evolution of a long-lived submarine channel system in the Late Cretaceous Nanaimo Group, British Columbia, Canada. *Sed. Geol.*, **337**, 113–132.

Beard, D.C. & Weyl, P.K. (1973) Influence of texture on porosity and permeability of unconsolidated sand. *AAPG Bull.*, **57**, 349–369.

Bjørlykke, K. (1993) Fluid flow in sedimentary basins. *Sed. Geol.*, **86**, 137–158.

Boehm, A. & Moore, J.C. (2002) Fluidized sandstone intrusions as an indicator of paleostress orientation, Santa Cruz, California. *Geofluids*, **2**, 147–161.

Bonham, L.C. (1980) Migration of hydrocarbons in compacting basins. *AAPG Bull.*, **64**, 549–567.

Brown, L.F., Benson, J.M., Brink, G.J., Doherty, S., Jollands, A., Jungslager, E.H.A., Keenan, J.H.G., Muntingh, A. & vanWyk, N.J.S. (1995) *Sequence Stratigraphy in Offshore South African Divergent Basins: An Atlas on Exploration for Cretaceous Lowstand Traps by Soekor (Pty) Ltd*, AAPG Studies in Geology, 41. AAPG, Tulsa, Oklahoma.

Brunt, R.L., Hodgson, D.M., Flint, S.S., Pringle, J.K., Di Celma, C., Prélat, A. & Grecula, M. (2013) Confined to unconfined: anatomy of a base of slope succession, Karoo Basin, South Africa. *Mar. Pet. Geol.*, **41**, 206–221.

Bureau, D., Mourges, R. & Cartwright, J. (2014) Use of a new artificial cohesive material for physical modelling: application to sandstone intrusions and associated fracture networks. *J. Struc. Geol.*, **66**, 223–236.

Cartwright, J. (2010) Regionally extensive emplacement of sandstone intrusions: a brief review. *Bas. Res.*, **22**, 502–516.

Catuneanu, O., Hancox, P.J. & Rubidge, B.S. (1998) Reciprocal flexural behaviour and contrasting stratigraphies: a new basin development model for the Karoo retroarc foreland system, South Africa. *Bas. Res.*, **10**, 417–439.

Chapman, R.E. (1987) Fluid flow in sedimentary basins: a geologist's perspective. In: *Fluid Flow in Sedimentary Basins and Aquifers* (Ed. by Goff J.C. & Williams B.P.J.) *Geol. Soc. Spec Publ.*, **34**, 3–18.

Cobain, S.L., Peakall, J. & Hodgson, D.M. (2015) Indicators of propagation direction and relative depth in clastic injectites: Implications for laminar versus turbulent flow processes. *GSA Bull.*, **127**, 1816–1830.

Cosgrove, J.W. (2001) Hydraulic fracturing during the formation and deformation of a basin: A factor in the dewatering of low-permeability sediments. *AAPG Bull.*, **85**, 737–748.

Di Celma, C.N., Brunt, R.L., Hodgson, D.M., Flint, S.S. & Kavanagh, J.P. (2011) Spatial and temporal evolution of a Permian submarine slope channel–levee system, Karoo Basin, South Africa. *J. Sed. Res.*, **81**, 579–599.

Diggs, T.N. (2007) An outcrop study of clastic injection structures in the Carboniferous Tesnus Formation, Marathon basin, Trans-Pecos Texas. In: *Sand Injectites: Implications for Hydrocarbon Exploration and Production* (Ed. by Hurst A. & Cartwright J.) *AAPG Mem.*, **87**, 209–219.

Dixon, R.J., Schofield, K., Anderton, R., Renolds, A.D., Alexander, R.W.S., Williams, M.C. & Davies, K.G. (1995) Sandstone diapirism and clastic intrusion in the Tertiary Submarine fans of the Bruce-Beryl Embayment, Quadrant 9, UKCS. In: *Characterization of Deep Marine Clastic Systems* (Ed. by Hartley A.J. & Prosser D.J.) *Geol. Soc. London. Spec. Publ.*, **94**, 77–94.

Duranti, D. (2007) Large-scale sand injection in the Paleogene of the North Sea: Modeling of energy and flow velocities. In: *Sand Injectites: Implications for Hydrocarbon Exploration and Production* (Ed. by Hurst A. & Cartwright J.) *AAPG Mem.*, **87**, 129–139.

Duranti, D. & Hurst, A. (2004) Fluidization and injection in the deep-water sandstones of the Eocene Alba Formation (UK North Sea). *Sedimentology*, **51**, 503–529.

Duranti, D., Hurst, A., Bell, C., Groves, B. & Hanson, R. (2002) Injected and remobilized Eocene sandstones from the Alba Field, UKCS: core and wireline log characteristics. *Pet. Geosci.*, **8**, 99–107.

Fildani, A., Drinkwater, N.J., Weislogel, A., McHargue, T., Hodgson, D.M. & Flint, S.S. (2007) Age controls on the Tanqua and Laingsburg deep-water systems: new insights on the evolution and sedimentary fill of the Karoo basin, South Africa. *J. Sediment. Res.*, **77**, 901–908.

Flemings, P.B., Stump, B.B., Finkbeiner, T. & Zoback, M. (2002) Flow focusing in overpressured sandstones: theory, observations, and applications. *American J. Sci.*, **302**, 827–855.

Flint, S.S., Hodgson, D.M., Sprague, A.R., Brunt, R.L., van der Merwe, W.C., Figueiredo, J., Prélat, A., Box, D., Di Celma, C. & Kavanagh, J.P. (2011) Depositional architecture and sequence stratigraphy of the Karoo basin floor to shelf edge succession, Laingsburg depocentre, South Africa. *Mar. Pet. Geol.*, **28**, 658–674.

Frey-Martínez, J., Cartwright, J., Hall, B. & Huuse, M. (2007) Sand Injectites: Implications for Hydrocarbon Exploration and Production. In: *Sand Injectites: Implications for Hydrocarbon Exploration and Production* (Ed. by Hurst A. & Cartwright J.) *AAPG Mem.*, **87**, 49–63.

Gardiner, A.R. (2006) The variability of turbidite sandbody pinchout and its impact on hydrocarbon recovery in stratigraphically trapped fields. In: *The Deliberate Search for the Stratigraphic Trap* (Ed. by Allen M.R.) *Geol. Soc. London. Spec. Publ.*, **254**, 267–287.

Gay, A., Takano, Y., Gilhooly, W.P. III, Berndt, C., Heeschen, K., Suzuki, N., Saegusa, S., Nakagawa, F., Tsunogai, U., Jiang, S.Y. & Lopez, M. (2011) Geophysical and geochemical evidence of large scale fluid flow within shallow sediments in the eastern Gulf of Mexico, offshore Louisiana. *Geofluids*, **11**, 34–47.

Halbouty, M.T. (1966) Stratigraphic-trap possibilities in Upper Jurassic rocks, San Marcos Arch, Texas. *AAPG Bull.*, **50**, 3–24.

Hamberg, L., Jepsen, A.M., Borch, N.T., Dam, G., Engkilde, M.K. & Svendsen, J.B. (2007) Mounded structures of injected sandstones in deep-marine Paleocene reservoirs, Cecile Field, Denmark. In: *Sand Injectites: Implications for Hydrocarbon Exploration and Production* (Ed. by Hurst A. & Cartwright J.) *AAPG Mem.*, **87**, 69–79.

Hiscott, R.N. (1979) Clastic sills and dikes associated with deep-water sandstones, Tourelle Formation, Ordovician, Quebec. *J. Sediment. Res.*, **49**, 1–9.

Hodgetts, D., Drinkwater, N.J., Hodgson, D.M., Kavanagh, J., Flint, S.S., Keogh, K.J. & Howell, J.A. (2004) Three-dimensional geological models from outcrop data using digital data collection techniques: an example from the Tanqua Karoo depocentre, South Africa. In: *Geological Prior Information Science and Engineering* (Ed. by Curtis A. & Wood R.) *Geol. Soc. London. Spec. Publ.*, **239**, 57–75.

Hodgson, D.M. (2009) Distribution and origin of hybrid beds in sand-rich submarine fans of the Tanqua depocentre, Karoo Basin, South Africa. *Mar. Pet. Geol.*, **26**, 1940–1956.

Hodgson, D.M., Flint, S.S., Hodgetts, D., Drinkwater, N.J., Johannessen, E.P. & Luthi, S.M. (2006) Stratigraphic evolution of fine-grained submarine fan systems, Tanqua Depocenter, Karoo Basin, South Africa. *J. Sediment. Res.*, **76**, 20–40.

Hodgson, D.M., Di Celma, C.N., Brunt, R.L. & Flint, S.S. (2011a) Submarine slope degradation and aggradation and the stratigraphic evolution of channel–levee systems. *J. Geol. Soc.*, **168**, 625–628.

Hodgson, D.M., van der Merwe, W.C. & Flint, S.S. (2011b) Distribution of submarine mass movement deposits: an exhumed basin perspective. In: *Advances in Natural and Technological Hazards Research - Submarine Mass Movements and Their Consequences*, 4th edn (Ed. by Y. Yamada, K. Kawamura, K. Ikehara, Y. Ogawa, R. Ureles, D. Mosher, J. Chaytor & M. Strasser), pp. 619–628. Springer, Netherlands.

Hodgson, D.M., Kane, I.A., Flint, S.S., Brunt, R.L. & Ortiz-Karpf, A. (2016) Time-transgressive confinement on the slope and the progradation of basin-floor fans: implications for the sequence stratigraphy of deep-water deposits. *J. Sediment. Res.*, **86**, 73–86.

Hofstra, M., Hodgson, D.M., Peakall, J. & Flint, S.S. (2015) Giant scour-fills in ancient channel-lobe transition zones: formative processes and depositional architecture. *Sed. Geol.*, **329**, 98–114.

Hofstra, M., Pontén, A.S.M., Peakall, J., Flint, S.S., Nair, K.N. & Hodgson, D.M. (2017) The impact of fine-scale reservoir geometries on streamline flow patterns in submarine lobe deposits using outcrop analogues from the Karoo Basin. *Petrol. Geosci.* doi:10.1144/petgeo2016-087

Hubbard, S.M., Romans, B.W. & Graham, S.A. (2007) An outcrop example of large-scale conglomeratic intrusions sourced from deep-water channel deposits, Cerro Toro Formation, Magallanes basin, southern Chile. In: *Sand Injectites: Implications for Hydrocarbon Exploration and Production* (Ed. by Hurst A. & Cartwright J.) *AAPG Mem.*, **87**, 199–207.

Hurst, A. & Cartwright, J.A. (2007) Relevance of sand injectites to hydrocarbon exploration and production. In: *Sand Injectites: Implications for Hydrocarbon Exploration and Production* (Ed. by Hurst A. & Cartwright J.) *AAPG Mem.*, **87**, 1–20.

Hurst, A., Cartwright, J., Huuse, M., Jonk, R., Schwab, A., Duranti, D. & Cronin, B. (2003) Significance of large-scale sand injectites as long-term fluid conduits: evidence from seismic data. *Geofluids*, **3**, 263–274.

Hurst, A., Scott, A. & Vigorito, M. (2011) Physical characteristics of sand injectites. *Earth-Sci. Rev.*, **106**, 215–246.

Huuse, M. & Mickelson, M. (2004) Eocene sandstone intrusions in the Tampen Spur area (Norwegian North Sea Quad 34) imaged by 3D seismic data. *Mar. Pet. Geol.*, **21**, 141–155.

Huuse, M., Duranti, D., Steinsland, N., Guargena, C.G., Prat, P., Holm, K., Cartwright, J.A. & Hurst, A. (2004) Seismic Characteristics of Large-Scale Sandstone Intrusions in the Paleogene of the South Viking Graben, UK and Norwegian North Sea. In: *3D Seismic Technology: Application to the Exploration of Sedimentary Basins* (Ed. by Davies R.J., Cartwright J.A., Stewart S.A., Lappin M. & Underhill J.R.) *Geol. Soc. London, Mem.*, **29**, 263–278. doi: 10.1144/GSL.MEM.2004.029.01.25

Huuse, M., Cartwright, J.A., Gras, R. & Hurst, A. (2005) Kilometre-scale sandstone intrusions in the Eocene of the Outer Moray Firth (UK North Sea): migration paths, reservoirs and potential drilling hazards. In: *Petroleum Geology: North-West Europe and Global Perspectives—Proceedings of the 6th Petroleum Geology Conference* (Ed. by A.G. Doré & B.A. Vining), pp. 1577–1594. Petroleum Geology Conferences Ltd. Geological Society, London.

Jackson, C.A.L. (2007) The Geometry, distribution, and development of clastic injections in slope systems: Seismic examples from the Upper Cretaceous Kyrre Formation, Mly Slope, Norwegian Margin. In: *Sand Injectites: Implications for Hydrocarbon Exploration and Production* (Ed. by Hurst A. & Cartwright J.) *AAPG Mem.*, **87**, 37–48.

Jackson, C., Huuse, M. & Barber, G. (2011) Geometry of winglike clastic intrusions adjacent to a deep-water channel complex: Implications for hydrocarbon exploration and production. *AAPG Bull.*, **95**, 559–584.

Jobe, Z.R., Lowe, D.R. & Morris, W.R. (2012) Climbing-ripple successions in turbidite systems: depositional environments, sedimentation rates and accumulation times. *Sedimentology*, **59**, 867–898.

Johnson, M.R. (1991) Sandstone petrography, provenance and plate tectonic setting in Gondwana context of the southeastern Cape-Karoo Basin. *South African J. Geol.*, **94**, 137–154.

Johnson, S.D., Flint, S.S., Hinds, D. & Wickens, H.Dev. (2001) Anatomy of basin floor to slope turbidite systems, Tanqua Karoo, South Africa: Sedimentology, sequence stratigraphy and implications for subsurface prediction. *Sedimentology*, **48**, 987–1023.

Johnson, M.R., Van Vuuren, C.J., Visser, J.N.J., Cole, D.I., Wickens, H.D.V., Christie, A.D.M., Roberts, D.L. & Brandl, G. (2006) Sedimentary rocks of the Karoo Supergroup. In: *The Geology of South Africa* (Ed. by M.R. Johnson, C.R. Anhaeusser, R.J. Thomas), pp. 461–499. Geological Society of South Africa, Johannesburg/Council for Geoscience, Pretoria.

Jolly, R.J.H. & Lonergan, L. (2002) Mechanisms and controls on the formation of sand intrusions. *J. Geol. Soc.*, **159**, 605–617.

Jones, G.E., Hodgson, D.M. & Flint, S.S. (2015) Lateral variability in clinoform trajectory, process regime, and sediment dispersal patterns beyond the shelf-edge rollover in exhumed basin margin-scale clinothems. *Basin Res.*, **27**, 657–680.

Jonk, R. (2010) Sand-rich injectites in the context of short-lived and long-lived fluid flow. *Basin Res.*, **22**, 603–621.

Jonk, R., Parnell, J. & Hurst, A. (2005a) Aqueous and petroleum fluid flow associated with sand injectites. *Basin Res.*, **17**, 241–257.

Jonk, R., Hurst, A., Duranti, D., Parnell, J., Mazzini, A. & Fallick, A.E. (2005b) Origin and timing of sand injection, petroleum migration, and diagenesis in Tertiary reservoirs, south Viking Graben, North Sea. *AAPG Bull.*, **89**, 329–357.

Jonk, R., Parnell, J. & Whitham, A. (2005c) Fluid inclusion evidence for a Cretaceous-Palaeogene petroleum system, Kangerlussuaq Basin, East Greenland. *Mar. Pet. Geol.*, **22**, 319–330.

Jonk, R., Duranti, D., Hurst, A., Parnell, J. & Fallick, A.E. (2007) Aqueous and petroleum fluids associated with sand injectites hosted by lacustrine shales from the oil-shale group (Dinantian), Midland Valley, Scotland. In: *Sand Injectites: Implications for Hydrocarbon Exploration and Production* (Ed. by Hurst A. & Cartwright J.) *AAPG Mem.*, **87**, 265–274.

Kane, I.A. (2010) Development and flow structures of sand injectites: the Hind Sandstone Member injectite complex, Carboniferous, UK. *Mar. Pet. Geol.*, **27**, 1200–1215.

Kane, I.A. & Hodgson, D.M. (2011) Sedimentological criteria to differentiate submarine channel levee subenvironments: exhumed examples from the Rosario Fm. (Upper Cretaceous) of Baja California, Mexico, and the Fort Brown Fm. (Permian), Karoo Basin, S. Africa. *Mar. Pet. Geol.*, **28**, 807–823.

Kelly, R.B., Houlsby, G.T. & Byrne, B.W. (2006) Transient vertical loading of model suction caissons in a pressure chamber. *Géotechnique*, **56**, 665–675.

King, R.C., Hodgson, D.M., Flint, S.S., Potts, G.J. & van Lente, B. (2009) Development of subaqueous fold belts as a control on the timing and distribution of deepwater sedimentation: an example from the southwest Karoo Basin, South Africa. In: *External Controls on Deep-Water Depositional Systems* (Ed. by Kneller B.C., Martinsen O.J. & McCaffrey W.) *SEPM Spec. Pub.*, **92**, 261–278.

Knipe, R.J., Jones, G. & Fisher, Q.J. (1998) Faulting, Fault Sealing and Fluid Flow in Hydrocarbon Reservoirs: an introduction. In: *Faulting, Fault Sealing and Fluid Flow in Hydrocarbon Reservoirs* (Ed. by Jones G., Fisher Q.J. & Knipe R.J.) *Geol. Soc. London. Spec. Publ.*, **147**, vii–xxi.

Krumbein, W.C. & Monk, G.D. (1942) Permeability as a function of the size parameters of unconsolidated sand. *Am. Inst. Min. Metall. Petrol. Eng. Tech. Publ.*, **1492**, 1–11.

Le Heron, D.P. & Etienne, J.L. (2005) A complex subglacial clastic dyke swarm, Sólheimajökull, southern Iceland. *Sed. Geol.*, **181**, 25–37.

Lonergan, L., Lee, N., Johnson, H.D., Cartwright, J.A. & Jolly, R.J. (2000) Remobilization and injection in deepwater depositional systems: Implications for reservoir architecture and prediction. In: *Deep-Water Reservoirs of the World* (Ed. by P. Weimer, R.M. Slatt, J. Coleman, N.C. Rosen, H. Nelson, A.H. Bouma, M.J. Styzen & D.T. Lawrence), pp. 515–532. GCSSEPM Foundation, 20th Annual Conference, Houston.

Lorenz, J.C., Teufel, L.W. & Warpinski, N.R. (1991) Regional fractures I: a mechanism for the formation of regional fractures at depth in flat-lying reservoirs. *AAPG Bull.*, **75**, 1714–1737.

Løseth, H., Raulline, B. & Nygård, A. (2013) Late Cenozoic geological evolution of the northern North Sea: development of a Miocene unconformity reshaped by large-scale Pleistocene sand intrusion. *J. Geol. Soc.*, **170**, 133–145.

Lunina, O.V. & Gladkov, A.S. (2015) Seismically induced clastic dikes as a potential approach for the estimation of the lower-bound magnitude/intensity of paleoearthquakes. *Eng. Geol.*, **195**, 206–213.

Luthi, S.M., Hodgson, D.M., Gell, C.R., Flint, S.S., Goedbloed, J.W., Drinkwater, N.J. & Johannessen, E.P. (2006) Con-tribution of research borehole data to modelling fine-grained turbidite reservoir analogues, Permian Tanqua-Karoo basin-floor fans (South Africa). *Pet. Geosci.*, **12**, 175–190.

Magara, K. (1981) Mechanisms of natural fracturing in a sedimentary basin. *AAPG Bull.*, **65**, 123–132.

Marchand, A.M.E., Apps, G., Li, W. & Rotzien, J.R. (2015) Depositional processes and impact on reservoir quality in deepwater Palaeogene reservoirs, US Gulf of Mexico. *AAPG Bull.*, **99**, 1635–1648.

McKay, M.P., Weislogel, A.L., Fildani, A., Brunt, R.L., Hodgson, D.M. & Flint, S.S. (2015) U-PB zircon tuff geochronology from the Karoo Basin, South Africa: implications of zircon recycling on stratigraphic age controls. *Int. Geol. Rev.*, **57**, 393–410.

van der Merwe, W.C., Flint, S.S. & Hodgson, D.M. (2010) Sequence stratigraphy of an argillaceous, deepwater basin-plain succession: vischkuil Formation (Permian), Karoo Basin, South Africa. *Mar. Pet. Geol.*, **27**, 321–333.

van der Merwe, W.C., Hodgson, D.M., Brunt, R.L. & Flint, S.S. (2014) Depositional architecture of sand-attached and sand-detached channel-lobe transition zones on an exhumed stepped slope mapped over a 2500 km^2 area. *Geosphere*, **10**, 1076–1093.

Minisini, D. & Schwartz, H. (2007) An early Paleocene cold seep system in the Panoche and Tumey Hills, central California (United States). In: *Sand Injectites: Implications for Hydrocarbon Exploration and Production* (Ed. by Hurst A. & Cartwright J.) *AAPG Mem.*, **87**, 185–197.

Monnier, D., Imbert, P., Gay, A., Mourgues, R. & Lopez, M. (2014) Pliocene sand injectites from a submarine lobe fringe during hydrocarbon migration and salt diapirism: a seismic example from the Lower Congo Basin. *Geofluids*, **14**, 1–19.

Morris, E.A., Hodgson, D.M., Brunt, R.L. & Flint, S.S. (2014) Origin, evolution and anatomy of silt-prone submarine external levées. *Sedimentology*, **61**, 1734–1763.

Morton, A., McFadyen, S., Hurst, A., Pyle, J. & Rose, P. (2014) Constraining the origin of reservoirs formed by sandstone intrusions: insights from heavy mineral studies of the Eocene in the Forties area, United Kingdom central North Sea. *AAPG Bull.*, **98**, 545–561.

Nagatomo, A. & Archer, S. (2015) Termination geometries and reservoir properties of the Forties Sandstone pinch-out, East Central Graben, UK North Sea. In: *Tertiary Deep-Marine Reservoirs of the North Sea* (Ed. by McKie T., Rose P.T.S., Hartley A.J., Jones D.W. & Armstrong T.L.) *Geol. Soc. London. Spec. Publ.*, **403**, 133–155.

Obermeier, S.F. (1996) Use of liquefaction-induced features for paleoseismic analysis—an overview of how seismic liquefaction features can be distinguished from other features and how their regional distribution and properties of source sediment can be used to infer the location and strength of Holocene paleo-earthquakes. *Eng. Geol.*, **44**, 1–76.

Obermeier, S.F., Oslon, S.M. & Green, R.A. (2005) Field occurrences of liquefaction-induced features: a primer for engineering geologic analysis of paleoseismic shaking. *Eng. Geol.*, **76**, 209–234.

Oliveira, C.M., Hodgson, D.M. & Flint, S.S. (2009) Aseismic controls on in situ soft-sediment deformation processes and products in submarine slope deposits of the Karoo Basin, South Africa. *Sedimentology*, **56**, 1201–1225.

Osborne, M.J. & Swarbrick, R.E. (1997) Mechanisms for generating overpressure in sedimentary basins: a reevaluation. *AAPG Bull.*, **81**, 1023–1041.

Palladino, G., Grippa, A., Bureau, D., Alsop, G.I. & Hurst, A. (2016) Emplacement of sandstone intrusions during contractional tectonics. *J. Struct. Geol.*, **89**, 230–249.

Parize, O. & Friès, G. (2003) The Vocontian clastic dykes and sills: a geometric model. In: *Subsurface Sediment Mobilization* (Ed. by Van Rensberge P., Hillis R.R., Maltman A.J. & Morley C.K.) *Geol. Soc. London. Spec. Publ.*, **216**, 51–72.

Peterson, G.L. (1966) Structural interpretation of sandstone dikes, Northwest Sacramento Valley, California. *GSA Bull.*, **77**, 833–842.

Prélat, A., Hodgson, D.M. & Flint, S.S. (2009) Evolution, architecture and hierarchy of distributary deep-water deposits: a high-resolution outcrop investigation from the Permian Karoo Basin, South Africa. *Sedimentology*, **56**, 2132–2154.

Richardson, J.F. (1971) Incipient fluidization and particulate systems. In: *Fluidization* (Ed. by J.F. Davidson, D. Harrison), pp. 25–64. Academic Press, London.

Ross, J.A., Peakall, J. & Keevil, G.M. (2014) Facies and flow regimes of sandstone-hosted columnar intrusions: insights from the pipes of Kodachrome Basin State Park. *Sedimentology*, **61**, 1764–1792.

Rowe, C.A., Mustard, P.S., Mahoney, J.B. & Katnick, D.C. (2002) Oriented clastic dike swarms as indicators of paleoslope? An example from the upper Cretaceous Nanaimo Group, Canada. *J. Sediment. Res.*, **72**, 192–200.

Schwab, A.M., Jameson, E.W. & Townsley, A. (2015) Volund Field: development of an Eocene sandstone injection complex, offshore Norway. In: *Tertiary Deep-Marine Reservoirs of the North Sea Region* (Ed. by McKie T., Rose P.T.S., Hartley A.J., Jones D.W. & Armstrong T.L.) *Geol. Soc. Lond. Spec. Publ.*, **403**, 247–260. doi:10.1144/SP403.4

Schwartz, H., Sample, J., Weberling, K.D., Minisini, D. & Moore, J.C. (2003) An ancient linked fluid migration system: cold-seep deposits and sandstone intrusions in the Panoche Hills, California, USA. *Geo-Mar. Lett.*, **23**, 340–350.

Scott, A., Vigorito, M. & Hurst, A. (2009) The process of sand injection: internal structures and relationships with host strata (Yellowbank Creek Injectite Complex, California, USA). *J. Sediment. Res.*, **79**, 568–583.

Shepherd, M., Kearney, C.J. & Milne, J.H. (1990) Magnus field. In: *Structural Traps II. Traps Associated With Tectonic Faulting* (Ed. by E.A. Beaumont & N.H. Foster), pp. 95–125. AAPG, Tulsa.

Sixsmith, P.J., Flint, S.S., Wickens, H.D. & Johnson, S.D. (2004) Anatomy and stratigraphic development of a basin floor turbidite system in the Laingsburg Formation, main Karoo Basin, South Africa. *J. Sediment. Res.*, **74**, 239–254.

Spychala, Y.T., Hodgson, D.M., Flint, S.S. & Mountney, N.P. (2015) Constraining the sedimentology and stratigraphy of submarine intraslope lobe deposits using exhumed examples from the Karoo Basin, South Africa. *Sed. Geol.*, **322**, 67–81.

Spychala, Y.T., Hodgson, D.M., Prélat, A., Kane, I.A., Flint, S.S. & Mountney, N.P. (2017) Frontal and lateral submarine lobe fringes: comparing sedimentary facies, architecture and flow processes. Accepted at *J. Sediment. Res.*, **87**, 1–21.

Stoker, S.J., Gray, J.C., Haile, P., Andrews, I.J. & Cameron, T.D.J. (2006) The importance of stratigraphic plays in the undiscovered resources of the UK Continental Shelf. In: *The Deliberate Search for the Stratigraphic Trap* (Ed. by Allen M.R.) *Geol. Soc. London. Spec. Publ.*, **254**, 153–167.

Sullivan, M., Jensen, G., Goulding, F., Jennette, D., Foreman, L. & Stern, D. (2000) Architectural analysis of deepwater outcrops: Implications for exploration and development of the Diana sub-basin, western Gulf of Mexico. In: *Deep-Water Reservoirs of the World: Gulf Coast Section SEPM Foundation 20th Annual Research Conference* (Ed. by Weimer P., Slatt R.M., Bouma A.H. & Lawrence D.T.), *SEPM CD Spec. Publ.*, **28**, 1010–1032.

Surlyk, F., Gjelberg, J. & Noe-Nygaard, N. (2007) The Upper Jurassic Hareelv Formation of east Greenland: a giant sedimentary injection complex. In: *Sand Injectites: Implications for Hydrocarbon Exploration and Production* (Ed. by Hurst A. & Cartwright J.) *AAPG Mem.*, **87**, 141–149.

Svendsen, J.B., Hansen, H.J., Stærmose, T. & Engkilde, M.K. (2010) Sand remobilization and injection above an active salt diapir: the Tyr sand of the Nini Field, Eastern North Sea. *Basin Res.*, **22**, 548–561.

Szarawarska, E., Huuse, M., Hurst, A., De Boer, W., Lu, L., Molyneux, S. & Rawlinson, P. (2010) Three-dimensional seismic characterisation of large-scale sandstone intrusions in the lower Palaeogene of the North Sea: completely injected vs. in situ remobilised sandbodies. *Basin Res.*, **22**, 517–532.

Tankard, A., Welsink, H., Aukes, P., Newton, R. & Stettler, E. (2009) Tectonic evolution of the Cape and Karoo basins of South Africa. *Mar. Pet. Geol.*, **26**, 1379–1412.

Truswell, J.F. (1972) Sandstone sheets and related intrusions from Coffee bay, Transkei, South Africa. *J. Sed. Res.*, **42**, 578–583.

Vétel, W. & Cartwright, J. (2010) Emplacement mechanics of sandstone intrusions: insights from the Panoche Giant Injection Complex, California. *Basin Res.*, **22**, 783–807.

Vigorito, M. & Hurst, A. (2010) Regional sand injectite architecture as a record of pore-pressure evolution and sand redistribution in the shallow crust: insights from the Panoche Giant Injection Complex, California. *J. Geol. Soc.*, **167**, 889–904.

Vigorito, M., Hurst, A., Cartwright, J. & Scott, A. (2008) Regional-scale subsurface sand remobilization: geometry and architecture. *J. Geol. Soc.*, **165**, 609–612.

Visser, J.N. & Praekelt, H.E. (1996) Subduction, mega-shear systems and Late Palaeozoic basin development in the African segment of Gondwana. *Geol. Rundsch.*, **85**, 632–646.

Von Brunn, V. & Talbot, C.J. (1986) Formation and deformation of subglacial intrusive clastic sheets in the Dwyka Formation of northern Natal, South Africa. *J. Sediment. Res.*, **56**, 35–44.

Walker, R.G. (1978) Deep-water sandstone facies and ancient submarine fans: models for exploration for stratigraphic traps. *AAPG Bull.*, **62**, 932–966.

van der Werff, W. & Johnson, S. (2003) High resolution stratigraphic analysis of a turbidite system, Tanqua Karoo Basin, South Africa. *Mar. Pet. Geol.*, **20**, 45–69.

Wickens, H.D. (1994) Basin floor fan building turbidites of the southwestern Karoo Basin, Permian Ecca Group, South Afrika. PhD thesis, University of Port Elizabeth, 233 pp.

Wickens, H.D. & Bouma, A.H. (2000) The Tanqua Fan Complex, Karoo Basin, South Africa—Outcrop analog for fine-grained, deepwater deposits. In: *Fine-Grained Turbidite Systems: American Association of Petroleum Geologists* (Ed. by Bouma A.H. & Stone C.G.) *Memoir*, **72** & SEPM Special Publication, 68, 153–165.

Wild, R., Flint, S.S. & Hodgson, D.M. (2009) Stratigraphic evolution of the upper slope and shelf edge in the Karoo Basin, South Africa. *Basin Res.*, **21**, 502–527.

Yang, S.Y. & Kim, J.W. (2014) Pliocene basin-floor fan sedimentation in the Bay of Bengal (offshore northwest Myanmar). *Mar. Pet. Geol.*, **49**, 45–58.

Yardley, G.S. & Swarbrick, R.E. (2000) Lateral transfer: a source of additional overpressure? *Mar. Pet. Geol.*, **17**, 523–537.

Manuscript received 21 January 2016; In revised form 18 December 2016; Manuscript accepted 19 December 2016.